Effects of Soluble Corn Fiber Consumption on Executive Functions and Gut Microbiota in Middle to Older Age Adults: A Randomized Controlled Crossover Trial

David A. Alvarado[1,4*], Tori A. Holthaus[1*], Shelby Martell[2], Nicole L. Southey[1], Marco Atallah[4], Rhea Sarma[3], David Revilla[4], Marina Brown[4], Twinkle Mehta[3], Naiman A. Khan[1,2,3,5], Hannah D. Holscher[1,4**]

[1]Division of Nutritional Sciences, University of Illinois Urbana-Champaign, Urbana, IL 61801, USA

[2]Neuroscience Program, University of Illinois Urbana-Champaign, Urbana, IL 61801, USA

[3]Health and Kinesiology, University of Illinois Urbana-Champaign, Urbana, IL 61801, USA

[4]Department of Food Science and Human Nutrition, University of Illinois Urbana-Champaign, Urbana, IL 61801, USA

[5]Beckman Institute of Advanced Science and Technology, Urbana-Champaign, Urbana, IL 61801, USA

[*]Shared first-authorship

[**]**Corresponding Author:** Hannah D. Holscher, 1201 West Gregory Drive, Urbana, IL 61801 (217) 300-2512, hholsche@illinois.edu

Hannah D. Holscher is an Editorial Board Member for *The Journal of Nutrition* and played no role in the Journal's evaluation of the manuscript.

Clinical Trial Registry: NCT05066425 (https://clinicaltrials.gov/study/NCT05066425)

Abbreviations: *Parabacteroides distasonis* (*P. distasonis*), Cambridge Neuropsychological Test Automated Battery (CANTAB), carbohydrate-active enzymes (CAZyme), Event-related potential (ERP), FDR (False Discovery Rate), Maltodextrin (CON, control), Perceived Stress Score (PSS), Positive and Negative Affect Schedule (PANAS), Profile of Moods Survey (POMS), Reaction Time (RT), SE (Standard Error), SEM (Standard Error of the Mean), Short-chain fatty acids (SCFA), Branched-chain fatty acids (BCFA), Soluble corn fiber/ PROMITOR® Soluble Fibre™ (SCF), Accuracy (ACC)

Abstract

Background: Dietary fiber may support cognition through gastrointestinal-microbiota mechanisms, but clinical evidence is limited.

Objectives: We aimed to determine whether soluble corn fiber (SCF) improved cognition and altered fecal microbiota and fermentation end products in adults.

Methods: In a randomized, double-blind, crossover trial, 42 healthy adults (45-75y) consumed SCF (18g/d) or a maltodextrin placebo control (CON: 22g/d) for 4 weeks, separated by a washout. Cognitive outcomes included executive function with event-related potentials, relational memory, neuropsychological performance, and mood. Secondary outcomes included fecal microbiota, metabolomics, and gastrointestinal tolerance. Tertiary analyses related microbial and metabolite changes to cognitive improvements using correlation, mediation, and moderation models, and explored SCF fermentation pathways with 16S-predicted functional profiling, shotgun metagenomics and *in vitro* culturing.

Results: SCF improved reaction times (RT) during congruent (β = -9.8 ms, 95% CI: [-18.4, -1.2], FDR P = 0.01) and incongruent (β = -14.2 ms, 95% CI: [-22.8, -5.6], FDR P = 0.003) flanker trials and increased *Parabacteroides* (~4-fold, β = 1.44 log, 95% CI [1.01, 1.88], FDR P < 0.001). At the SCF endpoint, congruent RT tended to be inversely associated with fecal acetate (ρ = -0.33) and propionate (ρ = -0.36), while *Parabacteroides* was marginally positively associated with acetate (ρ = 0.34) (all FDR P < 0.1). Moderation analyses indicated that SCF-RT relation varied by *Parabacteroides* magnitude change. At endpoint, SCF increased predicted functional potential of carbohydrate-related KOs and pathways (FDR P < 0.05). *In vitro* culturing confirmed *P. distasonis* ferments SCF.

Conclusion: SCF consumption improved attentional inhibition, altered the gut microbiota, and selectively enriched *Parabacteroides*. Although mediation analyses did not support a direct microbiota-to-cognition pathway, moderation analyses suggested that SCF-related cognitive effects may depend in part on *Parabacteroides* abundance. Collectively, these findings suggest that certain cognitive benefits of SCF consumption may be partly underpinned by the gut microbiota.

Keywords: Reaction time; Cognition; *Parabacteroides*; Gut-Brain; Dietary Fiber

Introduction

A healthy diet is a key determinant of metabolic health, and emerging evidence extends these benefits to brain function and cognition [1–3]. Dietary fiber is associated with reduced risk of obesity, cardiovascular disease, type 2 diabetes, and colon cancer [4,5], yet nearly 95% of Americans fail to meet recommended intake levels [6]. Further, dietary fiber provides a primary substrate for microbes residing in the gastrointestinal (GI) tract, shaping ecological community diversity and metabolic capacity [7]. Preclinical studies show that dietary fibers improve cognition [8,9], but human trials remain limited [10–12], particularly those linking the microbiota, GI-derived metabolites, and cognitive outcomes [13]. Therefore, further evidence is necessary to comprehensively characterize the effect of dietary fiber on general and specific domains of cognitive function.

Soluble corn fiber (SCF) is a resistant maltodextrin with an average degree of polymerization (DP) between 10-12 units [14], that supports glycemic control, calcium absorption, and gastrointestinal health [15–17]. Its non-viscous, water-soluble structure lacks β-linkages, yet branching of the α-linkages confers resistance to complete digestion in the small intestine (<30%) [18,19]. The undigested fraction undergoes colonic fermentation, enriching saccharolytic taxa such as *Bifidobacterium*, *Lactobacillus*, and *Parabacteroides* [20,21], and increasing short-chain fatty acids (SCFA) concentrations across age groups [22], while reducing deleterious fermentation end products (phenols, indoles, ammonia) [19,23]. SCFAs are increasingly recognized as key mediators of GI-brain communication by binding free fatty acid receptors (FFAR/FFAR3) to regulate immune [24] and enteroendocrine signaling [25], modulate microglial activity and systemic inflammation [26], and stimulate vagal and serotonergic pathways [27–30].

Executive functions, including inhibitory control, are central to attention, working memory, and flexible behavior [31]. These top-down processes can be assessed through computer-

99 based tasks that measure a subject's ability to maintain attention while faced with distracting
100 stimuli, hold and manipulate information in mind, and require multi-tasking and set-shifting, while
101 electrophysiological markers can provide complementary insight into neural activity during such
102 tasks [32,33]. Given the growing evidence that microbially derived metabolites influence brain
103 activity [27,34–39], assessing both behavioral and neural indices provides a comprehensive overview
104 to evaluate dietary fiber's cognitive impact.

105 To address these gaps, we conducted a randomized, double-blind, placebo-controlled,
106 crossover trial to test the impact of daily SCF consumption in middle- to older-aged adults. The
107 primary aim was to determine whether four weeks of SCF consumption improved executive
108 function, changes in the amplitude (size) and latency (timing) of the P3 event-related potential
109 (ERP), as well as additional behavioral tasks assessing relational memory and neuropsychological
110 function. We hypothesized that SCF would enhance cognitive control and reduce the number of
111 neural resources required to accomplish these cognitive processes. The secondary aim examined
112 the effects of SCF on fecal microbiota composition and fermentation metabolites, hypothesizing
113 that SCF consumption would enrich health-associated taxa and effect microbial-derived
114 metabolites. Finally, the tertiary aim tested whether the SCF-induced changes in microbial or
115 metabolite profiles explained changes in cognitive outcomes, hypothesizing that these changes
116 would contribute to the cognitive benefits induced by SCF.

117

118 **Methods**

119 *Study design and intervention*

120 This clinical trial, registered as the SCOPE study (Soluble Corn fiber for Promoting
121 Executive function; NCT05066425), included two 4-week intervention periods separated by an

122 ~4-week washout. Participants consumed soluble corn fiber (SCF; PROMITOR® Soluble Fibre™,
123 22g/d containing 18g fiber) or the maltodextrin placebo control (CON; 22g/d) in a counterbalanced
124 order. The two interventions were provided by Tate & Lyle in identical, pre-measured sachets that
125 were indistinguishable in taste and appearance. Sachets were labeled as 789 or 030, and
126 participants and research staff remained blinded to the code assignment until data analysis was
127 complete to ensure blinding. Participants were given 35 sachets per condition and were instructed
128 to consume one daily, dissolved in a fluid of their choice. Participants recorded intake of the sachet
129 on daily compliance logs. Unused sachets and logs were collected at the end of each period to
130 assess study adherence.

131 All study visits and testing sessions were conducted at the University of Illinois Urbana-
132 Champaign (Supplemental **Figure 1**). Anthropometric measures, physical activity level,
133 demographic information, and medical history were collected at baseline and visits 4, 5, and 6 as
134 potential covariates.

135

136 *Participants criteria*

137 Adults aged 45-75 years were recruited from the East Central Illinois area using email
138 newsletters, social media, community postings using the postal service, and flyers posted on public
139 transport. All participants were informed of all procedures and provided their written informed
140 consent before any data was collected. The SCOPE study was approved by the University of
141 Illinois Institutional Review Board (May 2021) and conducted following the principles of the
142 Declaration of Helsinki.

143 Exclusion criteria included physician-diagnosed gastrointestinal or metabolic disease
144 (inflammatory bowel disease and diabetes), neurological disorder (dementia, Parkinson's disease,

145 multiple sclerosis, brain tumors, autism), colorblindness or vision not corrected to 20/20, antibiotic
146 use within the past month, tobacco use, food allergies, pregnancy, or lactating, BMI <18.5 or >34.9
147 kg/m^2, Mini-Mental State Examination <24, or if habitual dietary fiber intake was >70% of the
148 daily recommended intake (≥18 g/d for women, ≥27 g/d for men) using the Dietary History
149 Questionnaire (*DHQ3*) food frequency questionnaire.

150 Eligible participants agreed to maintain habitual dietary patterns and physical activity, to
151 avoid probiotic or prebiotics supplements, and to report any changes in medications during the
152 SCOPE study.

153 Enrolled participants (**Table 1**) were randomized via coin toss to start one of the two
154 intervention conditions. Height and weight were measured in triplicate, without shoes and in light
155 clothing, to determine BMI using a *SECA* stadiometer (model 240; *SECA*, Hamburg, Germany)
156 and a Tanita WB-300 Plus digital scale (Tanita, Tokyo, Japan). Physical activity was assessed
157 using the Godin-Shephard Leisure-Time Exercise Questionnaire (*Godin*), which records the
158 frequency of strenuous, moderate, and light physical activities performed during a typical week,
159 which are totaled into a final score using a weighted formula [40].

160

161 **Aim 1: Cognitive Outcomes**

162 To minimize learning effects, participants completed practice sessions at the start of each
163 visit until at least 70% accuracy was met before experimental cognitive sessions were
164 administered. The order of cognitive task administration at each testing visit (visits 3-6) was
165 counterbalanced using a 2x2 Latin square design for each participant,

166 *Executive function*

167 Attentional inhibition was assessed using a modified Eriksen flanker task as previously
168 described [41]. Participants were asked to respond (*Current Designs*, Philadelphia, PA, USA) quickly
169 and accurately to the directionality of a central stimulus (3-cm tall white arrow) presented with
170 two flanking stimuli (arrows) on each side (83s stimulus presentation; 100ms response window;
171 jittered intertrial intervals of 1100, 1200, 1500ms). In congruent trial types, the flanking stimuli
172 matched the direction of the central arrow (<<<<<, >>>>>); during incongruent trials, flanking
173 stimuli opposed the central arrow (>><>>, <<>><<), requiring greater inhibitory control. The task
174 began with 40 practice trials followed by two blocks of 200 randomized experimental trials.
175 Behavioral measures were accuracy (ACC) and reaction time (RT) for correct responses.
176 Interference effects (flanker effect) for ACC and RT were calculated, respectively, by subtracting
177 incongruent from congruent measures (ACC) and congruent from incongruent measures (RT).
178 These measures index the ability to maintain task performance when resolving conflicting
179 information.
180
181 *Neuroelectric indices*
182 EEG activity was recorded simultaneously during the flanker task via a Neuro-scan Quik-
183 cap with 64 passive, wet, sintered Ag/AgCl scalp electrodes arranged in the international 10–10
184 system, with electrodes placed near the outside of each eye and above and below the left eye [42]. A
185 midline sensor placed between CZ and CPZ served as a reference, and AFZ served as the ground.
186 Continuous EEG data were digitized using a Neuroscan SynampsRT amplifier at a sampling rate
187 of 500 Hz, amplified 500 times to an online low-pass 70-Hz filter with a direct current and a 60-
188 Hz notch filter. Electrode impedance values were maintained at ≤20 kohms.

Signal processing was performed in MATLAB (MathWorks, Natick, MA, version 2021b) using EEGLab and ERPlab [43,44]. Continuous data were re-referenced to the average of two mastoid electrodes. A trained research team member visually inspected all channels for excessive noise during pre-processing. Channels with excessive noise were interpolated with an average of the adjacent electrodes. Data were submitted to a 0.1 Hz high-pass Butterworth filter before eye-blink artifacts were rejected using independent component analysis (ICA). ICA and vertical eye sensor channel correlations greater than 0.35 were considered eye-blinks. A time window of -200 to 1200 ms around stimulus presentation was used for creating stimulus-locked epochs with a baseline correction of -200 ms to stimulus onset. A 30-Hz low-pass filter was used. Artifacts were detected and rejected if a moving window peak-to-peak amplitude exceeded 100 μV, using a 100-ms window width and step. Only correct trials with >80% of artifact-free trials in all flanker task trials were retained, and participants with excessive artifacts (>20%) were excluded (n = 3 CON, n = 4 SCF), consistent with previous literature [45,46].

Electrodes of interest were chosen based on a collapsed localizer technique [47]. Evidence for selection was observed from maximal voltage localization of combined baseline and post-testing trials collapsed across condition and trial type. *Post-hoc* topographic average plots were constructed using a stylized topographic map plugin for EEGLAB/ERPLAB [48]. The P3 component was defined as the region of interest comprised of C1, CZ, C2, CPZ, CP1, and CP2 with a localized peak and corresponding latency between 300 and 600ms post-stimulus onset. Amplitude and latency were extracted to complement the analysis of the behavioral Flanker task.

Relational memory

211 Hippocampal-dependent relational memory was assessed using the computerized spatial
212 reconstruction task presentation software (*iPosition*; Neurobehavioral Systems, Berkeley, CA) [49].
213 Participants studied arrays of six abstract shapes on the computer screen in a randomized array for
214 6 seconds. The shapes were then masked by black squares for 18 seconds and could be revealed
215 individually by clicking on them. After a 2-second delay, the stimuli reappeared at the top of the
216 screen, and participants were asked to reconstruct the original array. Each participant completed
217 20 trials with randomized arrays. Two error metrics were used to assess performance:
218 misplacement error (original misplacement), calculated as the average measure of distance
219 between the actual and reconstructed stimuli locations, and object-location binding (accurate
220 single item placement), the number of times the participant correctly placed a stimulus within a
221 pre-defined radius.
222
223 *Neuropsychological battery*
224 Additional cognitive performance across multiple domains was assessed using the
225 Cambridge Neuropsychological Test Automated Battery (*CANTAB*, Cambridge Cognition Ltd)
226 [50,51], administered on a touchscreen tablet. The battery included the Intra-Extra Dimensional Set
227 Shift (IED), Stop Signal Task (SST), Rapid Visual Information Processing (RVP), and Spatial
228 Working Memory (SWM). The IED is a test which assesses rule acquisition and reversal,
229 attentional set formation, maintenance, and shifting. The RVP task assesses sustained attention,
230 and the SST measures response inhibition. The SWM task assesses spatial working memory.
231
232 *Mood and Stress*

233 Mood and stress were assessed using validated self-report instruments, including the
234 Profile of Mood States (*POMS*), the Positive and Negative Affect Schedule (*PANAS*), and the
235 Perceived Stress Scale (*PSS*). The *POMS* questionnaire includes 65-items that evaluates transient
236 mood states across six subscales (tension/anxiety, depression, anger, vigor, fatigue, and
237 confusion), with ratings from 0 ("not at all") to 5 ("extremely") [52,53]. *PANAS* includes 20 items
238 divided evenly into positive and negative affect subscales, scored from 1 ("very slightly or not at
239 all") to 5 ("extremely likely") [53,54]. *PSS-10* is a 10-item measure of stress over the past month,
240 scored from 0 ("never") to 4 ("very often") [55].
241
242 **Aim 2: Gut Microbiota and Metabolite Outcomes**
243 *Fecal collection and processing*
244 Participants provided two fecal samples at each of the four collection timepoints (baseline
245 and end of each of the two study conditions) for a total of 8 samples per participant. Samples were
246 collected during the five days preceding the first intervention and the final five days of each
247 treatment and washout period. Samples were delivered within 15 minutes of defecation using
248 provided kits (Commode Specimen Collection Systems, *Sage Products*) with ice packs and
249 coolers. Upon arrival at the laboratory, samples were homogenized, aliquoted into cryovials for
250 sequencing, flash-frozen in liquid nitrogen, and stored at -80°C. Additional aliquots were prepared
251 for metabolite analysis: SCFAs, BCFAs, ammonia, and dry matter basis (DMB; pre-weighed
252 aluminum tins). These aliquots were stored at -20°C until analysis. Fecal pH was measured
253 (*Denver Instrument*) after samples had been aliquoted.
254
255 *Fecal DNA isolation and 16S amplicon analyses*

256 Fecal microbial DNA was extracted using the Power-Lyzer PowerSoil DNA Isolation Kit
257 (*QIAGEN*). DNA was verified using 1% agarose gel electrophoresis, concentrations measured
258 using a Qbit 3.0 Fluorometer (*ThermoFisher Scientific*), quantified from two samples collected
259 per timepoint per participant, and pooled in equimolar amounts before sequencing at the University
260 of Illinois W.M Keck Center for Biotechnology. 16S Amplicons were generated with V4 primers
261 (*F*: 5'-GTGYCAGMGCCGCGGTAA, *R*: 5'-GGACTACNVGGGTWTCTAAT) [56] and
262 sequenced on an Illumina NovaSeq 6000 SP (2x250 nt), producing ~1 billion reads. Sequences
263 with quality scores >25 were processed with *DADA2* [57] integrated in *QIIME2* (v2023.7) [58].
264 Sequences were denoised and resolved into amplicon sequence variants (ASVs) using the *SILVA*
265 138-99 (515F/806R) naïve Bayes reference classifier [57,59]. Samples were normalized to 350,000
266 reads; curves plateaued at this depth, indicating adequate coverage (**Supplemental Figure 2**).
267 Rarefaction was performed with *vegan* v2.6.8 [60], filtering 1,521 ASVs (13%, primarily singletons
268 or zero-count features) and retaining 10,373 ASVs. Alpha diversity and beta diversity were
269 calculated with *phyloseq* (v1.48.0) [61], and Faith's phylogenetic diversity (Faith's PD) with *picante*
270 (v1.8.2). Taxonomic summaries were created at the genus and phylum levels for downstream
271 analyses.
272
273 *Targeted Metabolites*
274 Fecal dry matter was measured according to the Association of Official Analytical
275 Chemists, 1984, methods [62]. Ammonia concentrations were measured following the procedure of
276 Chaney and Marbach [63]. Aliquots for SCFA and BCFA were weighed, acidified with 2N
277 hydrochloric acid, and stored at -20°C until analysis. Briefly, SCFA (acetate, propionate, butyrate),
278 BCFA (isovalerate, valerate, and isobutyrate) concentrations were determined on the supernatant

279 fraction of the acidified fecal samples using gas chromatography mass spectroscopy (GC-MS).
280 Concentrations were calculated using standards[64]. Phenol and indole were quantified, according to
281 Flickinger et al.[65] Fecal metabolites are reported on the normalized DMB scale.
282
283 *Digestive health*
284 GI symptoms, bowel function, and stool characteristics were assessed using 7-day self-
285 reported records, questionnaires, and laboratory measures for each timepoint [66]. Participants rated
286 GI symptom severity (burping, cramping, bloating, gas, nausea, reflux, rumbling) on a 4-point
287 scale from 1 ("absent") to 4 ("severe") [67]. Bowel movements and consistency were scored using a
288 7-point Bristol stool scale (1- "separate hard lumps"; 2- "sausage-shaped but lumpy"; 3- "sausage-
289 like but with cracks on the surface"; 4- "sausage-like, smooth, and soft"; 5- "soft blobs with clear
290 cut edges"; 6- "fluffy pieces, mushy"; 7- "entirely liquid"). And ease of passage rated on a 5-point
291 scale from 1 ("very easy") to 5 ("very difficult"). In the laboratory, fresh fecal samples were
292 measured with a pH meter (Denver Instrument) [66], and a trained research team member recorded
293 stool consistency using the Bristol scale.
294
295 **Aim 3: Exploratory Integrative and Functional Analyses**
296 *Mediation and moderation*
297 Selected microbial and metabolite features for integrative analyses were prioritized from
298 Aim 1 and 2 outcomes that met the statistical significance threshold and were also included when
299 they showed consistent directional trends and biological plausibility based on prior literature [27,34–
300 39]. Associations between these candidates and cognitive outcomes were examined using Spearman
301 correlations. We then used nonparametric bootstrapped causal mediation models to estimate

302 indirect and direct effects within a causal inference framework [68–70]. Moderation analyses were
303 conducted using the Johson-Neyman framework with Aiken & West's simple-slopes procedures
304 [71,72]. Together, these complementary approaches will provide further clarity on whether microbes
305 or metabolites acted as intermediaries, transmitting the treatment (mediation), or as variables that
306 altered the strength or direction of the treatment's effect (moderation).
307
308 *In vitro isolated culturing*
309 *Parabacteroides distasonis* (*P. distasonis*), a species within the genus *Parabacteroides*
310 (strain 31_2, deposited as *Porphyromonas* sp. HM-169), was provided from the Biodefense and
311 Emerging Infections Research Resources Repository (BEI Resources, NIAID, NIH) and
312 maintained anaerobically in brain heart infusion (BHI) and chopped-meat broth. Growth assays
313 followed an adaptation of Garcia-Bayona et al. [73] using M9 supplemented with 50 mg/L L-
314 cysteine, 5 mg/L hemin, 2.5 µg/L vitamin K1, 2 mg/L FeSO4·7H2O, and 5 µg/L vitamin B12.
315 Treatments included glucose (0.25% wt/vol), CON (0.25% wt/vol), or SCF (0.4% wt/vol). BHI
316 served as a positive control; for negative controls, M9 with no carbon (no growth control), and
317 blanks (no inoculum) for each treatment (media contamination control). Stock solutions were
318 sterile-prepared, filter-sterilized (0.22 µm), and stored at 4 °C.
319 Three separate *P. distasonis* overnight cultures were inoculated into M9 solutions prepared
320 in a 10 x 10 honeycomb plate (1:10 dilution; starting OD_{600} = 0.1). For each treatment,
321 measurements were performed in technical triplicate across the 3 independent biological
322 replicates. Growth was monitored with the Bioscreen-C system (600nm, every 30 min, for 25.5h,
323 37°C, shaking before/after each read) (**Supplemental Figure 3**). All samples reached the

324 stationary phase by 14h; therefore, analyses were restricted to the first 14h. OD values were blank-
325 corrected and growth rates (μ) calculated at 2 h intervals.
326
327 *16S-inferred functional potential*
328 Predicted functional potential for the whole cohort was inferred from 16S data using
329 *PICRUSt2* (v2.5.3) [74] with default parameters (*picrust2_pipeline.py*) [74,75]. Predicted functions were
330 summarized as KEGG Orthologs (KOs) and pathways. *KEGGREST* (v112.1) was used to extract
331 carbohydrate metabolism pathways (map00010, 00030, 00500, 00620, 00650) and carbohydrate-
332 active KOs (KO01176, 01223, 01210, 01190, 01187, 012348). Stratified KO outputs were used to
333 quantify genus-level contributions to predicted functional differences across conditions.
334
335 *Responder shotgun metagenomics*
336 Participants from the whole cohort were classified based on their *Parabacteroides* response
337 to SCF using 16S genus-level relative abundance change (Δ = POST-PRE during the SCF period).
338 For an exploratory responder analysis, we selected a subset of six participants comprising the two
339 extremes in *Parabacteroides* responses to the SCF intervention period: three participants that
340 experienced the largest increases in *Parabacteroides* after the SCF intervention period
341 (responders, n=3) and the three participants that experienced the smallest changes in
342 *Parabacteroides* after the SCF intervention period (null or negative; non-responders, n=3).
343 Shotgun metagenomic sequencing of the extracted fecal DNA from the 3 responders and 3 non-
344 responders was conducted to assess species-level taxonomic profiles and exploratory beta-
345 diversity and functional patterns by responder status (**Supplemental Figure 4**).

346 Shotgun metagenomic sequencing was performed at the W. M. Keck Center for
347 Biotechnology (University of Illinois Urbana-Champaign). Libraries were pooled, quantified by
348 qPCR, and sequenced on half of a 10B lane for 151 cycles from both ends of the fragments using
349 a NovaSeq X Plus with V1.0 sequencing kits. FastQ files were demultiplexed (*bcl2fastq* v2.20),
350 adapters (CTGTCTCTTATACACATCT) were trimmed from the 3'-end of the reads, and base
351 quality scores were scored using Sanger encoding (*ASCII offset* of 33). Data pre-processing was
352 performed on the University cluster (Carl R. Woese Institute for Genomic Biology, University of
353 Illinois at Urbana-Champaign) using *KneadData* (v0.12.0) for quality control and host DNA
354 removal (*KneadData* 20230405 release). *Trimmomatic* (v0.39) removed low-quality bases,
355 *Tandem Repeat Finder* (TRF) removed noise from repetitive sequences, and *FastQC* (v0.11.9)
356 generated quality reports.

357 Following Huttenhower BioBakery pipelines [76–78], taxonomic profiling was performed
358 using *MetaPhlAn* (v4.0.6) [77], with *Bowtie2* (v2.5.0) aligning reads against the
359 *ChocoPhlAnSGB*_202212 reference. Functional profiles were generated using *HUMAnN* (v3.7) [76]
360 with the *ChocoPhlAn* nucleotide database (v201901b) and *UniRef90* protein database (Nov 2024).
361 Profiles were merged (*merge_metaphlan_tables.py*) to produce relative abundance and read counts
362 [77]. Descriptive analyses compared the log fold change between responders and non-responder's
363 delta values, retaining gene families with >2-fold change-targeted filtering for carbohydrate
364 metabolism-related terms yielded 217 candidate families. Carbohydrate-active enzymes
365 (CAZymes) were annotated using the CAZy database [79,80] and *run_dbcan* (v4.0.0)[81], incorporating
366 *HMMER* (*dbCAN_HMMdb)*, *DIAMOND* (CAZy protein sequences), and *dbCAN-sub* for substrate
367 prediction validated against PUL (Polysaccharide Utilization Loci) datasets. Reads were pre-
368 processed (*Trim Galore* v0.6.0, *Kraken2* v2.1.1), assembled into contigs ≥1000 bp (*MEGAHIT*

369 v1.2.9), and annotated with *Prokka* (v1.4) before CAZyme assignment. Clean reads were mapped
370 back to coding sequences (*BWA* v0.7.17-r1188, *Samtools* v1.7, *Bedtools* v2.27.1), and abundances
371 were normalized to transcripts per million (TPM) using *dbcan_utils* scripts [81]. Workflow was
372 conducted on a Linux computer (128 GB RAM) utilizing *Anaconda* (v23.7.3) environment.
373

374 **Statistical analyses**

375 *General approach.* Target enrollment was determined using *a priori* power calculations
376 (*G-Power* v3.1.9.2) [82], estimating that 36 participants would provide 80% power ($\beta = 0.80$) to
377 detect a small effect size ($r = 0.20$) at $\alpha = 0.05$ for Aims 1 and 2. Due to the exploratory nature of
378 Aim 3, results should be interpreted as hypothesis-generating and to inform effect size estimates
379 for future studies. To allow for attrition, 42 participants were recruited. Analyses were conducted
380 in *RStudio* (v2025.05.0+496; *R* v4.4.3) [83]. The significance threshold was set at $\alpha = 0.05$ with false
381 discovery rate (FDR) adjustments applied where relevant.

382 *Data preprocessing and assumptions.* Data distributions were checked using Shapiro-
383 Wilk's test (*stats* v4.4.3; $W > 0.9$), Q-Q plots (*ggplot2* v3.5.2) [84], skewness/kurtosis metrics
384 (*DescTools* v0.99.6*, e1071* v2.6*)*, and residuals inspected visually (*performance* v0.13.0). Extreme
385 outliers (>3 SD; *rstatix* v0.7.20) were confirmed using a Bonferroni *outlierTest* (*car* v3.1-3), then
386 winsorized [85,86]. To meet model assumptions, BCFAs POMS, PANAS, and Godin were square
387 root transformed; SCFAs were log-transformed. Data are reported as mean ± SEM unless
388 otherwise noted.

389 *Modeling strategy.* Outcomes were analyzed using linear (*lme4* v1.1.37) or generalized
390 (*glmmTMB* v1.1.11) mixed-effect models with treatment, time, and their interaction
391 (treatment:time) as fixed effects, and participant ID as a random intercept [*Outcome ~*

392 *Treatment*Time + (1|ID)*]. Order effects were tested and did not improve model fit, demonstrating
393 adequate washout time, therefore excluded. Missing data were not imputed; the mixed-effect
394 model provides valid estimates under the missing-at-random assumption [60]. We reported *p*-values,
395 estimates (β), standard errors (SE), and 95% confidence intervals (CI; *stats*) for the treatment effect
396 – the level of response attributable to the treatment – estimated by the treatment:time interaction
397 term, in the corresponding **Tables**. Fixed effects were evaluated using analysis of variance
398 (ANOVA; *car* v3.1-3). When the treatment:time term met the significance threshold, we
399 summarized simple-effects contrasts of estimated marginal means (*emmeans* v1.11.0), including
400 between-treatment comparisons at endpoint with Benjamini-Hochberg (FDR) corrections.
401 Baseline between-treatment contrasts were null across analyses. For outcomes with non-normal
402 residuals or otherwise not meeting model assumptions, we used paired Wilcoxon signed-rank tests.
403 *Aim 1*. All measures were analyzed with mixed-effects models (*lme4* v1.1.37). Flanker task
404 measures (ACC, RT, and interference scores) were tested using treatment-by-time models with
405 congruent and incongruent trial types evaluated separately. Two flanker ACC and two P3
406 amplitude outcomes were winsorized; *CANTAB* delta values were compared using paired
407 Wilcoxon Signed-rank tests.
408 *Aim 2*. 16S analyses utilized rarefied counts for normalization. Beta diversity was assessed
409 by PERMANOVA (*vegan* v2.6.10; 5,000 permutations) using participant ID as the permutation
410 stratum, with homogeneity of dispersion (*vegan*, 5,000 permutations) tested in parallel.
411 Differential abundance was assessed with negative binomial mixed-effect models (*glmmTMB*
412 v1.1.11) comparing a null [*Taxa ~ (1|ID)*] and full [*Taxa ~ Treatment*Time + (1|ID)*] model by a
413 likelihood ratio test across all included taxa [87–89]. Alpha diversity and fecal metabolites were

414 analyzed with mixed-effects models (*lme4* v1.1.37). Gastrointestinal symptoms were compared
415 with a paired Wilcoxon Signed-rank test.

416 *Aim 3*. *In vitro* growth rates across treatments were modeled using a linear model (*lm*) with
417 treatment, timepoint (every 2h), and the interaction as fixed effects, followed by pairwise contrasts
418 [90]. Predicted KO and pathway differences were compared with *MaAsLin2* (v1.18.0) [91] and
419 *ggpicrust2* (v2.0.0) [92]. Correlations between cognitive and microbial outcomes were assessed
420 using Spearman's rank correlation test (*stats* v4.4.3). Mediation analysis used baseline-adjusted
421 models to (1) predict the mediator from the Treatment [$\Delta Mediator \sim Treatment + Mediator_{Baseline}$]
422 and (2) predict the outcome from both the Treatment and the Mediator [$\Delta RT \sim Treatment *$
423 $\Delta Mediator + RT_{PRE}$]. Causal inference was estimated using nonparametric bootstrapping
424 (*mediation* v4.5.0; 8,000 simulations) with sensitivity analyses. Reported are the average causal
425 mediation effect (ACME), average direct effect (ADE), total effect, and proportion mediated.
426 Moderation models included treatment, a centered-scaled moderator (center="TRUE",
427 scale="TRUE"), and its interaction [$\Delta RT \sim Treatment * \Delta Moderator_{Z\text{-}Scaled}$]. Participant ID was
428 included as a random intercept, which caused model singularity; therefore, it was excluded.
429 Comparisons were probed using simple-slopes (*interactions* v1.2.0) and provided confidence
430 intervals (*emmeans* v1.11.0) at low (-1 SD), mean (0 SD), and high (+1 SD) changes of the
431 moderator.

432

433 Results

434 *Participant characteristics*

435 The CONSORT diagram (**Figure 1**) summarizes recruitment, enrollment, and retention.
436 Forty-two participants were randomized, of whom 41 completed the trial (**Table 1**). All

437 participants completed at least one cognitive testing visit, including one who withdrew after the
438 first intervention period (*n* = 1 CON). Per-protocol analyses included compliant participants who
439 consumed >80% of intervention sachets during at least one intervention period (Aim 1; *n* = 38
440 CON, 39 SCF). Ten participants had unusable P3 amplitude data (*n*=3 CON; 1 at pre, 2 at post
441 testing) and seven for the SCF (*n* = 2 PRE; *n* = 5 POST). Two participants could not provide fecal
442 samples but completed the primary cognitive aims (Aim 2; *n* = 38 CON, 37 SCF).
443
444 **Aim 1: Cognitive outcomes**
445 *Executive function*
446 Flanker task ACC remained high across the SCOPE study (≥ 92% scores), with ANOVA
447 showing no treatment effect (treatment:time) during congruent (P = 0.42) or incongruent trial
448 types (P = 0.53) (**Supplemental Figure 5**). RT exhibited a significant treatment effect during both
449 trials (congruent P = 0.01, incongruent P = 0.01). At endpoint, RT was faster following SCF in
450 both congruent (β = -9.8 ms, SE = 4.4, 95% CI: [-18.4, -1.2], FDR P = 0.01) and incongruent trials
451 (β = -14.2 ms, SE = 4.4, 95% CI: [-22.8, -5.6], FDR P = 0.003) (**Figure 2**). P3 distributions were
452 visualized (**Supplemental Figure 6**), no treatment effects were observed for P3 amplitudes
453 (congruent P = 0.46; incongruent P = 0.33) or peak latency (congruent P = 0.63; incongruent P
454 = 0.14). And no treatment effects were observed for interference scores of ACC (P = 0.10) or RT
455 (P = 0.39).
456
457 *Mood and Stress*
458 No treatment effects were observed for mood subscales and total mood disturbance scores
459 (*POMS*; all P > 0.53), relational memory performance (*iPosition*; all P > 0.45), affect scores

460 (*PANAS*; all $P > 0.45$), and stress (*PSS*-10; $P = 0.70$) (**Supplemental Table 1**). Similarly, no
461 treatment effects were observed across *CANTAB* measures (all $P > 0.13$) **(Supplemental Table**
462 **2-5**).
463
464 **Aim 2: Gut Microbiota and Metabolite Outcomes**
465 *16S Fecal microbiota*
466 Alpha diversity showed a treatment effect for observed richness (FDR $P = 0.03$), a
467 marginal effect for Faith's PD (FDR $P = 0.09$) and none for Shannon (FDR $P = 0.26$). Observed
468 richness was reduced following SCF at endpoint (β = -29.9 counts, SE = 8.55, 95% CI [-47.1, -
469 12.6], FDR $P = 0.01$) (**Table 5**; **Supplemental Figure 7)**. Beta diversity showed a small but
470 statistically significant treatment effect measured with Bray-Curtis (F = 0.81, $R^2 = 0.005$, FDR P
471 < 0.001), unweighted UniFrac (F = 0.47, $R^2 = 0.003$, FDR $P = 0.002$), and weighted UniFrac (F
472 = 1.07, $R^2 = 0.007$, FDR $P < 0.001$) (**Supplemental Figure 8)**. Endpoint comparisons with each
473 metric showed differences between SCF and CON for Bray-Curtis (F = 1.39, $R^2 = 0.019$, FDR P
474 < 0.001), unweighted UniFrac (F = 0.64, $R^2 = 0.010$, FDR $P = 0.005$), and weighted UniFrac (F
475 = 1.69, $R^2 = 0.023$, FDR $P < 0.001$).
476 At the phylum level, none met the significance threshold (**Supplemental Table 6**). A total
477 of 260 genera were detected, 128 passed filtering criteria (≥40% prevalence, >10 reads), and 14
478 met the significance threshold (all FDR $P < 0.05$); 11 were classified as low-abundance (<0.5%)
479 or as a group of bacteria without taxonomical assignment (incertae_sedis) (**Supplemental Table**
480 **7)**. *Parabacteroides* enrichment was consistently observed across 90% of participants during the
481 SCF arm (**Figure 3**), demonstrating a treatment effect ($\chi^2 = 42.0$, FDR $P < 0.001$)**,** with a ~4.1-
482 fold increase following SCF compared to CON (β = 1.44 log, SE = 0.16, 95% CI [1.01, 1.88], FDR

483 $P < 0.001$). *Fusicatenibacter* also showed a treatment effect ($\chi^2 = 17.94$, FDR $P < 0.001$) and
484 ~2.7-fold increase following SCF ($\beta = 1.10$ log, SE: 0.60, 95% CI: [0.59, 1.61], FDR $P < 0.001$).
485 Similarly, *Dialister* had a treatment effect ($\chi^2 = 7.25$, FDR $P = 0.02$) and increased by ~2.4-fold
486 following SCF ($\beta = 1.06$ log, SE: 0.39, 95% CI: [0.29, 1.83], FDR $P = 0.03$) (**Supplemental**
487 **Figure 9**).
488
489 *Targeted metabolites*
490 Fecal SCFAs (**Supplemental Figure 10**) and BCFAs did not statistically differ between
491 treatments (all $P > 0.14$; **Table 4**). Pooled total indoles (indole, 2-methylindole, 3-methylindole,
492 7-methylindole), indole, pooled total phenols (4-methylphenol, 4-ethylphenol, phenol), 4-
493 methylindole, and ammonia likewise did not show no treatment effect (all $P > 0.32$; **Supplemental**
494 **Table 8**).
495
496 *Gastrointestinal symptoms*
497 Symptom severity scores were generally absent to mild across conditions. No differences
498 were observed between SCF and CON for changes in cramping, nausea, reflux, rumbling, or
499 burping (all $P > 0.17$; **Table 5**). Flatulence (gas) severity scores increased following SCF ($P =$
500 0.01), although median severity remained <2 (mild) by endpoint (1.93 score). Bloating was
501 marginally increased following SCF ($P = 0.05$), though median scores remained 1.00 (absent). No
502 treatment effect was observed for self-reported feelings of consistency, ease of passage, bowel
503 frequency, or in the measured fecal pH (all $P > 0.22$; **Supplemental Table 9**).
504
505 **Aim 3: Exploratory Integrative and Functional Analyses**

506 Aim 3 analyses were restricted to primary cognitive outcomes that differed by treatment
507 (flanker RTs) and on the microbiota/metabolite features prioritized from Aim 2 based on either
508 evidence of SCF-responsiveness (*Parabacteroides*, *Fusicatenibacter*, and *Dialister*) or a
509 consistent directional trend with biological plausibility (acetate, propionate).

510 *Correlation analyses*

511 Spearman correlations at the SCF endpoint showed marginal inverse associations between
512 congruent RT and acetate (ρ = -0.33, FDR P = 0.09) and propionate (ρ = -0.36, FDR P = 0.09).
513 *Parabacteroides* was marginally associated with acetate (ρ = 0.34, FDR P = 0.09). No taxa were
514 associated with congruent RT (all FDR $P > 0.14$). For incongruent trials, no significant
515 correlations were detected with any candidate (all $\rho < 0.23$ and FDR $P > 0.30$) **(Supplementary**
516 **Figure 11)**.

517

518 *Mediation analyses*

519 The proportion mediated was estimated at ≤10.0% across candidates for congruent trials
520 and <4.1% for incongruent trials (**Table 6**). However, across candidates, indirect effects (ACME)
521 were not detected for either congruency (all $p \geq 0.19$), indicating no evidence of mediation.

522

523 *Moderation analyses*

524 Moderation models provided no evidence that candidate changes modified the treatment
525 effect on RT (all $P > 0.49$), except for *Parabacteroides*, which showed a moderation effect for
526 congruent (P = 0.05) and incongruent RTs (P = 0.04). Adding *Parabacteroides* increased
527 explained variance from ΔR^2 = 0.07 (base model) to ΔR^2 = 0.12 (adjusted), whereas other
528 candidates contributed <1% (**Table 7**).

529 For congruent trials, SCF-associated RT improvement depended on *Parabacteroides*
530 change (z-scored; 0 SD = average change): RT was faster when *Parabacteroides* changes were
531 small (-1SD: β = -29.5 ms, SE = 8.76, t = -3.37, 95% CI: [-47.0, -12.03], $P < 0.001$), but not when
532 *Parabacteroides* change was near the mean (0 SD; β = -9.7 ms, SE = 8.27, t = -1.18, 95% CI: [-
533 26.2, 6.8], $P = 0.24$) or much larger (+1 SD: β = 10.0 ms, SE = 16.27, t = 0.62, 95% CI: [-22.5,
534 42.5], $P = 0.54$). For incongruent trials, the treatment effect on RT similarly depended on
535 *Parabacteroides* change. RT was faster when changes were small (β = -32.4 ms, SE = 10.59, t = -
536 3.06, 95% CI: [-53.5, -11.2], $P < 0.001$), but not when change was near the mean (β = -7.30 ms,
537 SE = 10.0, t = -0.73, 95% CI: [-27.3, 12.7], $P = 0.47$) or much larger (β = 17.8 ms, SE = 19.68, t
538 = 0.90, 95% CI: [-21.5, 57.0], $P = 0.37$) (**Figure 4**).
539
540 *In vitro culturing of P. distasonis*
541 *P. distasonis* was confirmed to grow with SCF in isolation displaying a distinct growth
542 kinetics with significant media effect ($P < 0.001$), time ($P < 0.001$), and interaction ($P < 0.001$).
543 Growth on glucose and CON showed a short lag phase (<1h), and a rapid log phase reaching
544 stationary phase within 5-6h (glucose: OD_{600} = 0.59, 5.5h; CON: OD_{600} = 0.54, 5h). Growth on
545 SCF exhibited a two-phase diauxic growth pattern: a slower and smaller initial phase reaching
546 OD_{600} = 0.31 at 6h, followed by a ~2h lag, then a second log phase that peaked at OD_{600} = 0.61 by
547 14h. *Post-hoc* comparisons showed that SCF had significantly lower growth rates at 2h (all FDR
548 $P < 0.001$) and 4h (vs. glucose, FDR $P = 0.03$; vs. CON, FDR $P = 0.01$) relative to controls. By
549 6h, no differences were detected across treatments. At 8-10h, SCF had higher growth rates
550 compared to controls (all FDR $P < 0.001$), and remained higher at 12h (vs. glucose, FDR P =
551 0.002). By 14h, growth stabilized with no differences detected between treatments (**Figure 5)**.

552

553 *16S-Predicted functional potential analyses*

554 Predicted microbial pathway profiles from the full cohort indicated higher *N*-glycan
555 biosynthesis and α-linolenic acid metabolism pathways following SCF at endpoint compared to
556 control (all FDR $P < 0.01$). Predicted enzyme profiles (ECs) identified 23 functions differing by
557 treatment at endpoint (all FDR $P < 0.05$) (**Supplemental Figure 12**). MaAsLin2 detected 2,701
558 carbohydrate-metabolism KOs associated with SCF at endpoint (FDR $P < 0.05$). Among the top
559 SCF-associated KOs, 18 showed contribution by *Parabacteroides* (including glycan degradation
560 and complex carbohydrate utilization) and two by *Fusicatenibacter* (**Supplemental Figure 13**).

561

562 *Responder shotgun metagenomic analyses*

563 Metagenomic profile comparisons between responder vs. non-responded indicated no
564 differences in alpha diversity (all $P > 0.09$) or beta diversity. Responder status explained ~17% of
565 variance using Bray-Curtis PERMANOVA ($R^2 = 0.167$, $P = 0.05$), with no main effect of time
566 ($R^2 = 0.083$, $P = 0.44$) and no difference in the interaction ($R^2 = 0.079$, $P = 0.49$) (**Figure 6)**.
567 Metagenomic genus-level profiles focused on the treatment-responsive genera identified in 16S
568 analyses and confirmed that *Parabacteroides* was enriched in responders (Δ = 13.6%) and slightly
569 reduced in non-responders (Δ = -0.4%), consistent with 16S results. At the species level, *P.*
570 *distasonis* increased in responders (Δ = 10.9%) and remained non-detectable in non-responders,
571 while *P. merdae* also increased in responders (Δ = 2.7%) and decreased in non-responders (Δ = -
572 0.4%). *F. saccharivorans* negligibly increased in responders (Δ = 0.1%), compared to a larger
573 increase in non-responders (Δ = 2.2%). *D. hominis* (Δ = 1.4%) and *D. invisus* (0.3%) increased in
574 non-responder, while only *D. invisus* was detected and decreased in responders (Δ = -0.3%).

575 Functional analyses with *HUMAnN* showed an increase in carbohydrate metabolism-
576 related KOs among responders (UDP-glucose 6-dehydrogenase, α-amylases, hexokinase), while
577 non-responders demonstrated a lack of presence in these KOs (**Supplemental Figure 14**). Genus-
578 (**Supplemental Figure 15)** and species-level time comparisons (**Figure 10**) in responders
579 indicated increased contributions from *P. distasonis* to multiple carbohydrate-active gene families,
580 including glycoside hydrolases (GHs), α-amylases, and hexokinase. CAZy annotations provided
581 further resolution of GH families and subfamilies between groups. Of 228 GH families detected,
582 those with positive log fold changes in responders were isolated (**Supplemental Figure 16**).
583 Several GH families were enriched (GH43_8, GH43_33, GH25, GH24, GH179, GH13_9,
584 GH130_2, GH12) and positively correlated with *Parabacteroides* abundances (**Supplemental**
585 **Figure 17**).
586 Responders demonstrated faster RT across the SCF intervention for both congruent (Δ = -
587 0.90ms) and incongruent (Δ = 2.7ms) trials. In contrast, non-responders exhibited slower baseline
588 RT but demonstrated larger SCF-induced improvements (congruent Δ = -32.1ms, incongruent Δ
589 = -31.8ms). Parallel changes were observed in SCFAs; responders had higher baseline SCFA
590 levels and was increased in both groups for acetate (responders Δ = 66.4 vs. non-responders Δ =
591 71.6 μmol/g DMB) and propionate (responders Δ = 20.9 vs. non-responders Δ = 28.6 μmol/g
592 μmol/g DMB). (**Table 8**).
593
594 **Discussion**
595 In this randomized, double-blind, placebo-controlled, crossover trial, consuming SCF daily
596 for 4-weeks improved attentional inhibition, reflected by faster RT without compromising
597 accuracy on both congruent and incongruent flanker task trial types compared to control. Effects
598 were domain-specific to attentional inhibition, with no changes observed in relational memory,

599 rule acquisition and reversal, set shifting, sustained attention, response inhibition, or spatial
600 working memory observed (*Aim 1*). SCF consumption also shifted fecal microbial diversity,
601 selectively enriched *Parabacteroides*, numerically increased fecal acetate concentrations, and
602 produced absent-to-mild GI symptoms (*Aim 2*). SCF consumption had no effect on P3 amplitude
603 or latency, mood, or stress. Exploratory analyses did not identify any mediators but moderation
604 analyses suggested that SCF-related RT improvements varied by the magnitude of
605 *Parabacteroides* change. Consistent with 16S results identifying *Parabacteroides* as SCF-
606 responsive at the genus level, shotgun metagenomics identified *P. distasonis* as the primary SCF-
607 responsive species, while *in vitro* culturing independently confirmed its capacity to metabolize
608 SCF independent of cross-feeding (*Aim 3*).

609 Attentional inhibition is a core domain of cognitive control that can naturally and
610 insidiously decline with aging [31], underscoring the need for dietary strategies to preserve healthy
611 cognitive aging. Few clinical trials have assessed the impact of dietary fiber consumption on
612 cognition while integrating microbiome outcomes. The present work demonstrated that SCF
613 consumption selectively supported attentional inhibition, reflected by faster RT in congruent and
614 incongruent flanker trials, with no changes in other cognitive outcomes. This domain-specific
615 pattern reinforces the concept that gut-brain communication can influence higher-order cognitive
616 processes. Another randomized trial among 84 adults with overweight and obesity reported
617 improved accuracy, but no change in RT, during a modified flanker task following 12 weeks of
618 daily avocado consumption (12.8-16 grams fiber) relative to a control providing 3.2 – 4 grams
619 fiber daily [93]. Notably, avocado provides a mixed plant cell-wall fiber profile that is predominantly
620 insoluble (cellulose/hemicellulose) with soluble pectin (along with other nutrients) [94], whereas
621 SCF is a digestion-resistant maltodextrin dextrinized to produce a mixture of α-linkages (α-1,2, -

622 1,3, -1,4, and -1,6) [18,19], which may yield distinct fermentation kinetics and downstream signaling.
623 Specific to the microbiota, the avocado intervention increased α-diversity and
624 enriched *Faecalibacterium, Lachnospira*, and *Alistipes* and resulted in 18% greater fecal acetate,
625 concentrations due to fiber-rich avocado consumption [95]. Another nutrition trial reported mood
626 benefits with 16 g/day inulin for 12 weeks versus 16 g maltodextrin among adults with obesity,
627 particularly among individuals exhibiting a specific microbial signature, however, no effects were
628 observed on inhibitory control, working memory, or cognitive flexibility regardless of changes in
629 the gut microbiota [39]. Inulin is a β(2,1)-linked fructan (fructose polymer), whereas SCF is glucose
630 based [96,97]. Other lifestyle interventions, such as increased physical activity, have been shown to
631 improve flanker RT after a single exercise session, with one randomized trial among 106 healthy-
632 weight adults showing improvements in both congruent (458 ms vs 475 ms) and incongruent (528
633 ms vs 547 ms) paradigms immediately following 30 min of high-intensity aerobic exercise
634 compared with seated rest [98]. Collectively, these studies suggest that cognition effects are domain-
635 and context-specific, shaped by factors such as fiber type, population characteristics, physical
636 activity status, and intervention duration, which complicates direct cross-study comparisons but
637 underscores nutrition as a potential modifiable factor for cognitive health. However, the fiber type
638 (e.g., SCF, pectin), host and microbiome characteristics, and exposure duration needed to exact
639 cognitive benefits is yet to be delineated, highlighting the need for additional robust clinical trials.
640 Our work demonstrated that *Parabacteroides* was enriched following SCF consumption,
641 which is consistent with previous SCF supplementation trials. Specifically, a randomized dose-
642 responsive trial with free-living pubertal females (0, 10, and 20g fiber/d, 4 weeks per dose), a
643 randomized double-blind trial with healthy adults (20 g/d; 10 days per period), and a randomized
644 double-blind trial with only healthy adult men (21 g/d; 21 days per period) all reported enrichment

645 of *Parabacteroides* [21,99,100]. In the present study, SCF consumption reduced observed richness at
646 endpoint, which has been previously reported with fermentable fibers when selective utilization
647 leads to an increase of a narrower set of taxa and a more dominated community structure, without
648 necessarily indicating an adverse effect [101] as shown by its consistent role as a fermentable and
649 generally well tolerated fiber [97].

650 The convergence of 16S with the full cohort and shotgun metagenomes on responder subset
651 supports the robustness of the *Parabacteroides* enrichment across sequencing approaches. In
652 responders, *P. distasonis* abundance was inversely related to *Bacteroides vulgatus*, suggesting
653 possible ecological competition under SCF exposure. Predicted functional profiles and shotgun
654 metagenomics indicated increased carbohydrate metabolism pathways and glycan degradation
655 capacity, with CAZy highlighting an increased in *Parabacteroides*-associated GHs (GH35, GH43,
656 and GH73) [102,103]. *P. distasonis*-specific GHs (GH144 and GH13) involved in the hydrolysis α-
657 glycosidic bonds were also detected [102,103]. CAZymes serving similar functions are typically
658 organized within PULs, gene clusters that coordinate sensing, import, and degradation of dietary
659 glycans [104]. The enrichment of these CAZymes likely reflects an activation of SCF-targeting PULs,
660 enabling *P. distasonis* to maintain a competitive niche in the large intestine. Our *in vitro*
661 experiment supported this metabolic capacity, showing that *P. distasonis*, with no prior SCF
662 exposure, fermented SCF in a diauxic pattern, consistent with the mixture of fiber and non-fiber
663 starches in the formula. Together, these findings position *Parabacteroides* as a primary degrader
664 of SCF, although mechanistic insights remain limited.

665 These findings are consistent with the ISAPP definition of a prebiotic: "a substrate that is
666 selectively utilized by host microorganisms, conferring a health benefit" [105]. SCF induced small
667 shift in the GI microbiota, selectively increasing *Parabacteroides*, and provided a cognitive benefit

668 in healthy older adults. *Parabacteroides* responded to SCF in 90% of the healthy cohort, consistent
669 with the 'Health-Associated Core Keystone' (HACK) index which identified *P. distasonis, P.*
670 *merdae*, and *F. saccharivorans* as core and stability-associated taxa [106]. Prior work links *P.*
671 *distasonis* with anti-inflammatory effects, gut barrier protection [107–109], and bioactive metabolite
672 production (e.g., GABA)[110], relevant to gut-brain communication and health outcomes [102,111,112].
673 Although *Parabacteroides* did not directly mediate cognitive benefits in the SCOPE study, its
674 consistent response to SCF suggests its potential role as a keystone taxon in healthy older adults.

675 In this study, fecal SCFA concentration differences did not reach statistical significance;
676 however, their directional changes align with prior dietary fiber interventions and remain plausible
677 candidates for gut-brain signaling, given their ability to cross and modulate the blood-brain
678 barrier's structural integrity [34,35,113–116]. Notably, fecal SCFA concentrations in the present study
679 were lower than those reported in a younger, male-only SCF trial using a higher dose (21g/d) [19],
680 which may reflect differences in participant characteristics such transit time, absorption, and/or
681 dilution with greater stool mass. Prior human studies show that colonic SCFA delivery influences
682 anticipatory brain reward responses and attenuates cortisol reactivity to psychosocial stress [35].
683 Despite biological plausibility, in the present study, mediation and moderation models did not
684 support fecal SCFAs as either mediators or moderators of the SCF effect.

685 Moderation analyses suggested that the SCF effect on RT varied with the magnitude of
686 change in *Parabacteroides*. RT improvements were greatest at smaller *Parabacteroides* changes
687 (-1SD), whereas larger *Parabacteroides* changes were not associated with faster RTs.
688 Furthermore, responders consistently performed quicker at baseline and endpoints, while non-
689 responders exhibited larger improvements from SCF for RT speeds. These exploratory findings

690 suggest that *Parabacteroides* may exert a context-dependent influence, but its enrichment may not
691 be linearly beneficial for cognitive performance.

692 Secondary taxa provided additional exploratory context for the SCF-RT association.
693 Although mediation models did not support Dialister or *Fusicatenibacter* as intermediaries of the
694 SCF effect on RT, their descriptive patterns were informative. Bacillota members such as
695 *Fusicatenibacter* are capable of cross-feeding on substrates released by members of the
696 Bacteroidota phylum [117] (e.g., *Parabacteroides*), producing beneficial metabolites including
697 acetate, lactate, formate, and succinate [118]. Potentially, *Fusicatenibacter* may have had the role of
698 the main secondary consumer working with *Parabacteroides* in response to SCF. Responders had
699 higher baseline levels of *F. saccharivorans* which showed negligible enrichment with SCF,
700 whereas non-responders exhibited a relatively larger enrichment in *F. saccharivorans*. In contrast,
701 *D. invisus* and *D. hominis* were enriched only in non-responders and remained below detectable
702 levels in responders. A prior study linked *Fusicatenibacter saccharivorans* with executive and
703 visuospatial functions with community-dwelling older adults [119], whereas *Dialister invisus* was
704 reported to be more abundant in older adults with mild cognitive impairment [119]. Together, these
705 patterns suggest that baseline community composition and differential responsiveness may
706 contribute to cognitive variability, though mechanistic inferences remain preliminary.

707 The SCOPE study has several limitations. First, the cohort was predominantly white,
708 female, and highly educated, which may restrict generalizability. Mediation and moderation
709 analysis were exploratory and did not fully account for the crossover design in its statistical
710 framework and utilized change and baseline adjustments. Shotgun metagenomic analyses were
711 limited to a small subset of responders and non-responders, reducing power to detect subtle effects.
712 The absence of blood samples prevented assessment of circulating SCFAs or other metabolites,

713 while the targeted fecal metabolomics panel may have overlooked additional relevant compounds
714 (e.g., tryptophan catabolites). Furthermore, fecal SCFAs can be influenced by colonic transit time
715 and may only reflect a fraction *in vivo* production. Systemic inflammatory markers and neuroactive
716 metabolites were not assessed and should be incorporated in future mechanistic trials. Although
717 participants agreed to maintain their habitual diets, inter-individual dietary variation may have
718 introduced unmeasured noise into microbiome and metabolite outcomes. Despite these limitations,
719 the SCOPE study provides novel evidence linking SCF to selective cognitive benefits, supported
720 by exploratory insights into microbial and SCFA response.

721 In conclusion, daily consumption of SCF for four weeks improved RT in middle aged and
722 older adults and induced a microbiota shift dominated by *Parabacteroides*. Exploratory
723 moderation suggested a threshold effect, with RT benefits most evident at smaller changes in
724 *Parabacteroides*. Notably, cognitive improvements were also observed in non-responders with
725 negligible *Parabacteroides*, indicating that cognitive benefits are unlikely to hinge on a single
726 taxon but may instead depend on the ecological context and balance between health associated
727 keystone microbes (e.g., *Parabacteroides* and *Fusicatenibacter*) for contributing complementary
728 routes to induce GI-brain interactions [120]. Host factors may also contribute to interindividual
729 variability in cognitive response to SCF. These findings position SCF as a dietary fiber with
730 potential cognitive relevance, while underscoring the need for multi-omics, untargeted
731 metabolomics, dosing trials, and systemic biomarker assessments to refine mechanistic models
732 and advance precision nutrition strategies for cognitive health.

733

734

735

Acknowledgments

We thank Dr. Michael J. Miller for his expertise, equipment, and facility to conduct the *in vitro* culturing experiment. We also thank Dr. Pratik Banerjee and his graduate students (Papri Suraya Rahman and Edwin Valenzuela De Leon) for providing the *P. distasonis* strain and assisting with the equipment set-up. We are also grateful to the HDH graduate students: Alexis Baldeon, Marahi Perez-Tamayo, Nadine Veasly, and Maria Sanabria-Veaz; HDH staff: Eva Cornman, Myra Esmail, Karen Gutierrez, and Tehila Abdiel; and NAK graduate students Shelby Keyes and John Kim, as well as the undergraduate research assistants from HDH and NAK laboratories, for their assistance during the appointments, sample processing, and data management.

Author Contributions

HDH, NAK, DAA and TAH: designed the research; MDB and TM: recruited and enrolled participants and coordinated study procedures; DAA: conducted the *in vitro* experiment; DAA, TAH, SM, TM and RS: conducted the experiments and testing appointments; MA, DR and DAA: managed biological samples collection and storages; DAA and TAH: managed study data; DAA and NS: prepared data for bioinformatic pipelines; DAA and TAH: analyzed the data: DAA, TAH, NAK and HDH: wrote the manuscript; NAK and HDH: had primary responsibility for final content. All authors read and approved the final manuscript.

Author Disclosures: The authors report no conflict of interest.

Funding: This work was supported by Tate & Lyle Ingredients Americas LLC (to NAK) and the USDA NIFA, Hatch Project (1026591, to HDH).

Data Availability: Data described in the manuscript, code book, and analytic code will be made available upon request.

759 **References**
760

761 1. Morris MC, Wang Y, Barnes LL, Bennett DA, Dawson-Hughes B, Booth SL. Nutrients
762 and bioactives in green leafy vegetables and cognitive decline: Prospective study.
763 *Neurology*. 2018;90(3):E214-E222. doi:10.1212/WNL.0000000000004815
764 2. Perim Baldo M, Aboussaleh Y, Turrini A, et al. Adherence to a Mediterranean-Style Diet
765 and effects on Cognition in Adults: A Qualitative evaluation and Systematic Review of
766 Longitudinal and Prospective Trials. 2016;3:1. doi:10.3389/fnut.2016.00022
767 3. Khan NA, Raine LB, Donovan SM, Hillman CH. IV. The cognitive implications of
768 obesity and nutrition in childhood. *Monogr Soc Res Child Dev*. 2014;79(4):51-71.
769 doi:10.1111/mono.12130
770 4. Cho SS, Qi L, Fahey GC, Klurfeld DM. Consumption of cereal fiber, mixtures of whole
771 grains and bran, and whole grains and risk reduction in type 2 diabetes, obesity, and
772 cardiovascular disease. *American Journal of Clinical Nutrition*. 2013;98(2):594-619.
773 doi:10.3945/ajcn.113.067629
774 5. Trock B, Lanza E, Greenwald P, Lanza E, Greenwald P. *REVIEW Dietary Fiber,*
775 *Vegetables, and Colon Cancer: Critical Review and Meta-Analyses of the Epidemiologic*
776 *Evidence*. https://academic.oup.com/jnci/article/82/8/650/882222
777 6. Gov D. *Dietary Guidelines for Americans Make Every Bite Count With the Dietary*
778 *Guidelines*. https://www.
779 7. Marchesi JR, Ravel J. The vocabulary of microbiome research: a proposal. *Microbiome*.
780 2015;3(1). doi:10.1186/s40168-015-0094-5
781 8. Fleming SA, Monaikul S, Patsavas AJ, Waworuntu R V., Berg BM, Dilger RN. Dietary
782 polydextrose and galactooligosaccharide increase exploratory behavior, improve
783 recognition memory, and alter neurochemistry in the young pig. *Nutr Neurosci*.
784 2019;22(7):499-512. doi:10.1080/1028415X.2017.1415280
785 9. Gronier B, Savignac HM, Miceli M Di, et al. Increased cortical neuronal responses to
786 NMDA and improved attentional set-shifting performance in rats following prebiotic (B-
787 GOS s) ingestion. doi:10.1016/j.euroneuro.2017.11.001
788 10. Khan NA, Raine LB, Drollette ES, Scudder MR, Kramer AF, Hillman CH. Dietary Fiber
789 Is Positively Associated with Cognitive Control among Prepubertal Children. *J Nutr*.
790 2015;145(1):143-149. doi:10.3945/JN.114.198457
791 11. Hassevoort KM, Lin AS, Khan NA, Hillman CH, Cohen NJ. Added sugar and dietary
792 fiber consumption are associated with creativity in preadolescent children. *Nutr Neurosci*.
793 2020;23(10):791-802. doi:10.1080/1028415X.2018.1558003
794 12. Naveed S, Venäläinen T, Eloranta AM, et al. Associations of dietary carbohydrate and
795 fatty acid intakes with cognition among children. *Public Health Nutr*. 2020;23(9):1657-
796 1663. doi:10.1017/S1368980019003860
797 13. Cryan JF, O KJ, M Cowan CS, et al. The Microbiota-Gut-Brain Axis. *Physiol Rev*.
798 2019;99:1877-2013. doi:10.1152/physrev.00018.2018.-The
799 14. Stewart ML, Nikhanj SD, Timm DA, Thomas W, Slavin JL. Evaluation of the effect of
800 four fibers on laxation, gastrointestinal tolerance and serum markers in healthy humans.
801 *Ann Nutr Metab*. 2010;56(2):91-98. doi:10.1159/000275962
802 15. Shuan W, Tan K, Fen P, et al. The Role of Soluble Corn Fiber on Glycemic and Insulin
803 Response. doi:10.3390/nu12040961

16. Jakeman SA, Henry CN, Martin BR, et al. Soluble corn fiber increases bone calcium retention in postmenopausal women in a dose-dependent manner: A randomized crossover trial. *American Journal of Clinical Nutrition*. 2016;104(3):837-843. doi:10.3945/ajcn.116.132761
17. Klosterbuer AS, Hullar MAJ, Li F, et al. Gastrointestinal effects of resistant starch, soluble maize fibre and pullulan in healthy adults. doi:10.1017/S0007114513000019
18. LinAmy AHM, Nichols BL, Quezada-Calvillo R, et al. Unexpected high digestion rate of cooked starch by the Ct-maltase-glucoamylase small intestine mucosal α-glucosidase subunit. *PLoS One*. 2012;7(5). doi:10.1371/journal.pone.0035473
19. Vester Boler BM, Rossoni Serao MC, Bauer LL, et al. Digestive physiological outcomes related to polydextrose and soluble maize fibre consumption by healthy adult men. *British Journal of Nutrition*. 2011;106(12):1864-1871. doi:10.1017/S0007114511002388
20. Maathuis A, Venema K, Hoffman A, Evans A, Sanders L. The effect of the undigested fraction of maize products on the activity and composition of the microbiota determined in a dynamic in vitro model of the human proximal large intestine. *J Am Coll Nutr*. 2009;28(6):657-666. doi:10.1080/07315724.2009.10719798
21. Whisner CM, Martin BR, Nakatsu CH, et al. Soluble corn fiber increases calcium absorption associated with shifts in the gut microbiome: A randomized dose-response trial in free-living pubertal females. *Journal of Nutrition*. 2016;146(7):1298-1306. doi:10.3945/jn.115.227256
22. Arroyo MC, Laurie I, Rotsaert C, Marzorati M, Risso D, Karnik K. Age-Dependent Prebiotic Effects of Soluble Corn Fiber in M-SHIME® Gut Microbial Ecosystems. *Plant Foods for Human Nutrition*. 2023;78(1):213-220. doi:10.1007/s11130-023-01043-z
23. Holscher HD, Gregory Caporaso J, Hooda S, Brulc JM, Fahey GC, Swanson KS. Fiber supplementation influences phylogenetic structure and functional capacity of the human intestinal microbiome: Follow-up of a randomized controlled trial. *American Journal of Clinical Nutrition*. 2015;101(1):55-64. doi:10.3945/ajcn.114.092064
24. Brown AJ, Goldsworthy SM, Barnes AA, et al. The orphan G protein-coupled receptors GPR41 and GPR43 are activated by propionate and other short chain carboxylic acids. *Journal of Biological Chemistry*. 2003;278(13):11312-11319. doi:10.1074/jbc.M211609200
25. Cani PD, Lecourt E, Dewulf EM, et al. Gut microbiota fermentation of prebiotics increases satietogenic and incretin gut peptide production with consequences for appetite sensation and glucose response after a meal. *American Journal of Clinical Nutrition*. 2009;90(5):1236-1243. doi:10.3945/ajcn.2009.28095
26. Corrêa-Oliveira R, Fachi JL, Vieira A, Sato FT, Vinolo MAR. Regulation of immune cell function by short-chain fatty acids. *Clin Transl Immunology.John Wiley and Sons Inc.* 2016;5(4). doi:10.1038/cti.2016.17
27. Dalile B, Van Oudenhove L, Vervliet B, Verbeke K. The role of short-chain fatty acids in microbiota–gut–brain communication. *Nat Rev Gastroenterol Hepatol.Nature Publishing Group*. 2019;16(8):461-478. doi:10.1038/s41575-019-0157-3
28. Zhou SY, Guo ZN, Yang Y, Qu Y, Jin H. Gut-brain axis: Mechanisms and potential therapeutic strategies for ischemic stroke through immune functions. *Front Neurosci.Frontiers Media S.A.* 2023;17. doi:10.3389/fnins.2023.1081347

29. Silva YP, Bernardi A, Frozza RL. The Role of Short-Chain Fatty Acids From Gut Microbiota in Gut-Brain Communication. *Front Endocrinol (Lausanne).Frontiers Media S.A.* 2020;11. doi:10.3389/fendo.2020.00025
30. Mansuy-Aubert V, Ravussin Y. Short chain fatty acids: the messengers from down below. *Front Neurosci*. 2023;17. doi:10.3389/fnins.2023.1197759
31. Diamond A. Executive functions. *Annu Rev Psychol.Annual Reviews Inc.* 2013;64:135-168. doi:10.1146/annurev-psych-113011-143750
32. Duncan-Johnson CC. P300 latency: A new metric of information processing. *Psychophysiology*. 1981;18(3):207-215. doi:10.1111/j.1469-8986.1981.tb03020.x
33. Polich J. Updating P300: An integrative theory of P3a and P3b. *Clinical Neurophysiology*. 2007;118(10):2128-2148. doi:10.1016/j.clinph.2007.04.019
34. La Torre D, Verbeke K, Dalile B. Dietary fibre and the gut–brain axis: microbiota-dependent and independent mechanisms of action. *Gut Microbiome*. 2021;2. doi:10.1017/gmb.2021.3
35. Dalile B, Fuchs A, La Torre D, Vervliet B, Van Oudenhove L, Verbeke K. Colonic butyrate administration modulates fear memory but not the acute stress response in men: A randomized, triple-blind, placebo-controlled trial. *Prog Neuropsychopharmacol Biol Psychiatry*. 2024;131. doi:10.1016/j.pnpbp.2024.110939
36. Cheng J, Hu H, Ju Y, et al. Gut microbiota-derived short-chain fatty acids and depression: deep insight into biological mechanisms and potential applications. *Gen Psychiatr.BMJ Publishing Group*. 2024;37(1). doi:10.1136/gpsych-2023-101374
37. Luqman A, He M, Hassan A, et al. Mood and microbes: a comprehensive review of intestinal microbiota's impact on depression. *Front Psychiatry.Frontiers Media SA*. 2024;15. doi:10.3389/fpsyt.2024.1295766
38. Haskell CF, Scholey AB, Jackson PA, et al. Cognitive and mood effects in healthy children during 12 weeks' supplementation with multi-vitamin/minerals. *British Journal of Nutrition*. 2008;100(5):1086-1096. doi:10.1017/S0007114508959213
39. Leyrolle Q, Cserjesi R, D.G.H. Mulders M, et al. Prebiotic effect on mood in obese patients is determined by the initial gut microbiota composition: A randomized, controlled trial. *Brain Behav Immun*. 2021;94:289-298. doi:10.1016/j.bbi.2021.01.014
40. Godin-Leisure-Time-Exercise-Questionnaire_070815.
41. Edwards CG, Walk AM, Cannavale CN, et al. Dietary choline is related to neural efficiency during a selective attention task among middle-aged adults with overweight and obesity. *https://doi.org/101080/1028415X20191623456*. 2019;24(4):269-278. doi:10.1080/1028415X.2019.1623456
42. Chatrian GE, Lettich E, Nelson PL. American Journal of EEG Technology Ten Percent Electrode System for Topographic Studies of Spontaneous and Evoked EEG Activities Ten Percent Electrode System for Topographic Studies of Spontaneous and Evoked EEG Activities. Published online 2015. doi:10.1080/00029238.1985.11080163
43. Delorme A, Makeig S. EEGLAB: An open source toolbox for analysis of single-trial EEG dynamics including independent component analysis. *J Neurosci Methods*. 2004;134(1):9-21. doi:10.1016/J.JNEUMETH.2003.10.009
44. Lopez-Calderon J, Luck SJ. ERPLAB: An open-source toolbox for the analysis of event-related potentials. *Front Hum Neurosci*. 2014;8(1 APR):213. doi:10.3389/FNHUM.2014.00213/BIBTEX

45. Kamijo K, Pontifex MB, Khan NA, et al. The association of childhood obesity to neuroelectric indices of inhibition. *Psychophysiology*. 2012;49(10):1361-1371. doi:10.1111/J.1469-8986.2012.01459.X
46. Walk AM, Edwards CG, Baumgartner NW, et al. The role of retinal carotenoids and age on neuroelectric indices of attentional control among early to middle-aged adults. *Front Aging Neurosci*. 2017;9(JUN):183. doi:10.3389/FNAGI.2017.00183/BIBTEX
47. Luck SJ, Gaspelin N. How to get statistically significant effects in any ERP experiment (and why you shouldn't). *Psychophysiology*. 2017;54(1):146-157. doi:10.1111/PSYP.12639
48. Pontifex MB. Stylized Topographic Map Plugin for EEGLAB/ERPLAB.
49. Horecka KM, Dulas MR, Schwarb H, Lucas HD, Duff M, Cohen NJ. Reconstructing relational information. *Hippocampus*. 2018;28(2):164-177. doi:10.1002/hipo.22819
50. Langley C, Sahakian B, Robbins T. Cambridge neuropsychological test automated battery (cantab). *SAGE Publications Ltd*. 2023;0:435-468.
51. Wild K V., Musser ED. The cambridge neuropsychological test automated battery in the assessment of executive functioning. In: *Handbook of Executive Functioning*. Springer New York; 2014:171-190. doi:10.1007/978-1-4614-8106-5_11
52. Stephen J. Gibson. The Measurement of Mood States in Older Adults. *The Journals of Gerontology: Series B*. 1997;52B(4):167-174.
53. Boyle GJ, Helmes E, Matthews G, Izard CE. Measures of Affect Dimensions. In: *Measures of Personality and Social Psychological Constructs*. Elsevier Inc.; 2015:190-224. doi:10.1016/B978-0-12-386915-9.00008-5
54. Humboldt S von, Monteiro A, Leal I. Validation of the PANAS: A Measure of Positive and Negative Affect for Use with Cross-National Older Adults. *Rev Eur Stud*. 2017;9(2):10. doi:10.5539/res.v9n2p10
55. Lee EH. Review of the psychometric evidence of the perceived stress scale. *Asian Nurs Res (Korean Soc Nurs Sci)*. 2012;6(4):121-127. doi:10.1016/j.anr.2012.08.004
56. Walters W, Hyde ER, Berg-Lyons D, et al. Improved Bacterial 16S rRNA Gene (V4 and V4-5) and Fungal Internal Transcribed Spacer Marker Gene Primers for Microbial Community Surveys. *mSystems*. 2016;1(1). doi:10.1128/msystems.00009-15
57. Callahan BJ, McMurdie PJ, Rosen MJ, Han AW, Johnson AJA, Holmes SP. DADA2: High-resolution sample inference from Illumina amplicon data. *Nat Methods*. 2016;13(7):581-583. doi:10.1038/nmeth.3869
58. Bolyen E, Rideout JR, Dillon MR, et al. Reproducible, interactive, scalable and extensible microbiome data science using QIIME 2. *Nat Biotechnol.Nature Publishing Group*. 2019;37(8):852-857. doi:10.1038/s41587-019-0209-9
59. Yilmaz P, Parfrey LW, Yarza P, et al. The SILVA and "all-species Living Tree Project (LTP)" taxonomic frameworks. *Nucleic Acids Res*. 2014;42(D1). doi:10.1093/nar/gkt1209
60. Morton JT, Marotz C, Washburne A, et al. Establishing microbial composition measurement standards with reference frames. *Nat Commun*. 2019;10(1). doi:10.1038/s41467-019-10656-5
61. McMurdie PJ, Holmes S. Phyloseq: An R Package for Reproducible Interactive Analysis and Graphics of Microbiome Census Data. *PLoS One*. 2013;8(4). doi:10.1371/journal.pone.0061217
62. Kenneth Helrich. *Official Methods for Analysis of the Association of Official Analytical Chemists*.; 1990.

63. Chaney AL, MEP. Modified Reagents for Determination of Urea and Ammonia. *Clin Chem*. 1962;8(2):130-132.
64. Holscher HD, Doligale JL, Bauer LL, et al. Gastrointestinal tolerance and utilization of agave inulin by healthy adults. *Food Funct*. 2014;5(6):1142-1149. doi:10.1039/c3fo60666j
65. Flickinger EA, Schreijen EMWC, Patil AR, et al. Nutrient digestibilities, microbial populations, and protein catabolites as affected by fructan supplementation of dog diets Get access Arrow. *J Anim Sci*. 2003;81(8):2008-2018.
66. Holscher HD, Chumpitazi BP, Dahl WJ, et al. Perspective: Assessing Tolerance to Nondigestible Carbohydrate Consumption. *Advances in Nutrition*. 2022;13(6):2084-2097. doi:10.1093/advances/nmac091
67. Maki K, Rains T, Kelley K, Cook C, Schild A, Gietl E. Fibermalt is well tolerated in healthy men and women at intakes up to 60 g/d: a randomized, double-blind, crossover trial. *Int J Food Sci Nutr*. 2013;63(3):274-281.
68. Tingley D, Yamamoto T, Hirose K, Keele L, Imai K. *Journal of Statistical Software Mediation: R Package for Causal Mediation Analysis*.; 2014. http://www.jstatsoft.org/
69. Chi WE, Huang S, Jeon M, Park ES, Melguizo T, Kezar A. A Practical Guide to Causal Mediation Analysis: Illustration With a Comprehensive College Transition Program and Nonprogram Peer and Faculty Interactions. *Front Educ (Lausanne)*. 2022;7. doi:10.3389/feduc.2022.886722
70. Sohn MB, Li H. Compositional mediation analysis for microbiome studies. *Annals of Applied Statistics*. 2019;13(1):661-681. doi:10.1214/18-AOAS1210
71. Aiken LS, West SG. Interaction Effects. In: *Encyclopedia of Statistics in Behavioral Science*. Wiley; 2005. doi:10.1002/0470013192.bsa306
72. Preacher KJ, Curran PJ, Bauer DJ. *Computational Tools for Probing Interactions in Multiple Linear Regression, Multilevel Modeling, and Latent Curve Analysis*. Vol 31.; 2006. http://www.quantpsy.org/.437
73. García-Bayona L, Comstock LE. Streamlined genetic manipulation of diverse bacteroides and parabacteroides isolates from the human gut microbiota. *mBio*. 2019;10(4). doi:10.1128/mBio.01762-19
74. Douglas GM, Maffei VJ, Zaneveld JR, et al. PICRUSt2 for prediction of metagenome functions. *Nat Biotechnol.Nature Research*. 2020;38(6):685-688. doi:10.1038/s41587-020-0548-6
75. Langille MGI, Zaneveld J, Caporaso JG, et al. Predictive functional profiling of microbial communities using 16S rRNA marker gene sequences. *Nat Biotechnol*. 2013;31(9):814-821. doi:10.1038/nbt.2676
76. Beghini F, McIver LJ, Blanco-Míguez A, et al. Integrating taxonomic, functional, and strain-level profiling of diverse microbial communities with biobakery 3. *Elife*. 2021;10. doi:10.7554/eLife.65088
77. Blanco-Míguez A, Beghini F, Cumbo F, et al. Extending and improving metagenomic taxonomic profiling with uncharacterized species using MetaPhlAn 4. *Nat Biotechnol*. 2023;41(11):1633-1644. doi:10.1038/s41587-023-01688-w
78. Segata N, Izard J, Waldron L, et al. Metagenomic biomarker discovery and explanation. *Genome Biol*. 2011;12(6). doi:10.1186/gb-2011-12-6-r60

79. Drula E, Garron ML, Dogan S, Lombard V, Henrissat B, Terrapon N. The carbohydrate-active enzyme database: Functions and literature. *Nucleic Acids Res*. 2022;50(D1):D571-D577. doi:10.1093/nar/gkab1045
80. Cantarel BI, Coutinho PM, Rancurel C, Bernard T, Lombard V, Henrissat B. The Carbohydrate-Active EnZymes database (CAZy): An expert resource for glycogenomics. *Nucleic Acids Res*. 2009;37(SUPPL. 1). doi:10.1093/nar/gkn663
81. Zheng J, Ge Q, Yan Y, Zhang X, Huang L, Yin Y. DbCAN3: Automated carbohydrate-Active enzyme and substrate annotation. *Nucleic Acids Res*. 2023;51(W1):W115-W121. doi:10.1093/nar/gkad328
82. Erdfelder E, FAul F, Buchner A, Lang AG. Statistical power analyses using G*Power 3.1: Tests for correlation and regression analyses. *Behav Res Methods*. 2009;41(4):1149-1160. doi:10.3758/BRM.41.4.1149
83. R Core Team. R: A language and environment for statistical computing. *Foundation for Statistical Computing*. Preprint posted online 2013.
84. H. Wickham. ggplot2: Elegant Graphics for Data Analysis. *Springer-VerlagNew York*. Published online 2016.
85. Kwak SK, Kim JH. Statistical data preparation: Management of missing values and outliers. *Korean J Anesthesiol.Korean Society of Anesthesiologists*. 2017;70(4):407-411. doi:10.4097/kjae.2017.70.4.407
86. Kafadar K. John Tukey and Robustness. *Statistical Science*. 2003;3(18(3)):319-331. doi:1076102419
87. Zhang X, Mallick H, Tang Z, et al. Negative binomial mixed models for analyzing microbiome count data. *BMC Bioinformatics*. 2017;18(1). doi:10.1186/s12859-016-1441-7
88. Sweeny AR, Lemon H, Ibrahim A, et al. A mixed-model approach for estimating drivers of microbiota community composition and differential taxonomic abundance. *mSystems*. Published online July 25, 2023. doi:10.1128/msystems.00040-23
89. Jamieson PE, Smart EB, Bouranis JA, et al. Gut enterotype-dependent modulation of gut microbiota and their metabolism in response to xanthohumol supplementation in healthy adults. *Gut Microbes*. 2024;16(1). doi:10.1080/19490976.2024.2315633
90. Zwietering MH, Jongenburger I, Rombouts FM, Van ' K, Riet T. *Modeling of the Bacterial Growth Curve PUm*.; 1990. https://journals.asm.org/journal/aem
91. Mallick H, Rahnavard A, McIver LJ, et al. Multivariable association discovery in population-scale meta-omics studies. *PLoS Comput Biol*. 2021;17(11). doi:10.1371/journal.pcbi.1009442
92. Yang C, Mai J, Cao X, Burberry A, Cominelli F, Zhang L. ggpicrust2: an R package for PICRUSt2 pre-dicted functional profile analysis and visualiza-tion. *Bioinformatics, YYYY*.:0-0. doi:10.1093/bioinformatics/xxxxx
93. Edwards CG, Walk AM, Thompson S V., et al. Effects of 12-week avocado consumption on cognitive function among adults with overweight and obesity. *International Journal of Psychophysiology*. 2020;148:13-24. doi:10.1016/j.ijpsycho.2019.12.006
94. Ford NA, Spagnuolo P, Kraft J, Bauer E. Nutritional Composition of Hass Avocado Pulp. *Foods.Multidisciplinary Digital Publishing Institute (MDPI)*. 2023;12(13). doi:10.3390/foods12132516
95. Thompson S V., Bailey MA, Taylor AM, et al. Avocado Consumption Alters Gastrointestinal Bacteria Abundance and Microbial Metabolite Concentrations among

Adults with Overweight or Obesity: A Randomized Controlled Trial. *Journal of Nutrition*. 2021;151(4):753-762. doi:10.1093/jn/nxaa219

96. Fda. *Review of the Scientific Evidence on the Physiological Effects of Certain Non-Digestible Carbohydrates*.; 2018.

97. Mysonhimer AR, Holscher HD. Gastrointestinal Effects and Tolerance of Nondigestible Carbohydrate Consumption. *Advances in Nutrition*. 2022;13(6):2237-2276. doi:10.1093/advances/nmac094

98. Mehren A, Luque CD, Brandes M, et al. Intensity-dependent effects of acute exercise on executive function. *Neural Plast*. 2019;2019. doi:10.1155/2019/8608317

99. Timm DA, Thomas W, Boileau TW, Williamson-Hughes PS, Slavin JL. Polydextrose and soluble corn fiber increase five-day fecal wet weight in healthy men and women. *Journal of Nutrition*. 2013;143(4):473-478. doi:10.3945/jn.112.170118

100. Hooda S, Vester Boler BM, Rossoni Serao MC, et al. 454 pyrosequencing reveals a shift in fecal microbiota of healthy adult men consuming polydextrose or soluble corn fiber. *Journal of Nutrition*. 2012;142(7):1259-1265. doi:10.3945/jn.112.158766

101. Cantu-Jungles TM, Hamaker BR. Tuning Expectations to Reality: Don't Expect Increased Gut Microbiota Diversity with Dietary Fiber. *Journal of Nutrition*. 2023;153(11):3156-3163. doi:10.1016/j.tjnut.2023.09.001

102. Shimizu H, Nakajima M, Miyanaga A, et al. Characterization and Structural Analysis of a Novel exo-Type Enzyme Acting on β-1,2-Glucooligosaccharides from Parabacteroides distasonis. *Biochemistry*. 2018;57(26):3849-3860. doi:10.1021/acs.biochem.8b00385

103. Ducarmon QR, Karcher N, Tytgat HLP, et al. Large-scale computational analyses of gut microbial CAZyme repertoires enabled by Cayman. Preprint posted online January 8, 2024. doi:10.1101/2024.01.08.574624

104. Lapébie P, Lombard V, Drula E, Terrapon N, Henrissat B. Bacteroidetes use thousands of enzyme combinations to break down glycans. *Nat Commun*. 2019;10(1). doi:10.1038/s41467-019-10068-5

105. Gibson GR, Hutkins R, Sanders ME, et al. Expert consensus document: The International Scientific Association for Probiotics and Prebiotics (ISAPP) consensus statement on the definition and scope of prebiotics. *Nat Rev Gastroenterol Hepatol.Nature Publishing Group*. 2017;14(8):491-502. doi:10.1038/nrgastro.2017.75

106. Goel A, Shete O, Goswami S, et al. Toward a health-associated core keystone index for the human gut microbiome. *Cell Rep*. 2025;44(3):115378. doi:10.1016/j.celrep.2025.115378

107. Cui Y, Zhang L, Wang X, et al. Roles of intestinal Parabacteroides in human health and diseases. *FEMS Microbiol Lett.Oxford University Press*. 2022;369(1). doi:10.1093/femsle/fnac072

108. Cuffaro B, Boutillier D, Desramaut J, et al. Characterization of Two Parabacteroides distasonis Candidate Strains as New Live Biotherapeutics against Obesity. *Cells*. 2023;12(9). doi:10.3390/cells12091260

109. Ezeji JC, Sarikonda DK, Hopperton A, et al. Parabacteroides distasonis: intriguing aerotolerant gut anaerobe with emerging antimicrobial resistance and pathogenic and probiotic roles in human health. *Gut Microbes.Bellwether Publishing, Ltd.* 2021;13(1). doi:10.1080/19490976.2021.1922241

110. Liang Z, Di N, Li L, Yang D. Gut microbiota alterations reveal potential gut–brain axis changes in polycystic ovary syndrome. *J Endocrinol Invest*. 2021;44(8):1727-1737. doi:10.1007/s40618-020-01481-5
111. Wei W, Wong CC, Jia Z, et al. Parabacteroides distasonis uses dietary inulin to suppress NASH via its metabolite pentadecanoic acid. *Nat Microbiol*. 2023;8(8):1534-1548. doi:10.1038/s41564-023-01418-7
112. Liu D, Zhang S, Li S, et al. Indoleacrylic acid produced by Parabacteroides distasonis alleviates type 2 diabetes via activation of AhR to repair intestinal barrier. *BMC Biol*. 2023;21(1). doi:10.1186/s12915-023-01578-2
113. Keaney J, Campbell M. The dynamic blood-brain barrier. *FEBS Journal*. 2015;282(21):4067-4079. doi:10.1111/febs.13412
114. Van Dokkum W, Wezendonk B, Srikumar TS, Van Den Heuvel EGHM. Effect of nondigestible oligosaccharides on large-bowel functions, blood lipid concentrations and glucose absorption in young healthy male subjects. *Eur J Clin Nutr*. 1999;53(1):1-7. doi:10.1038/sj.ejcn.1600668
115. Pedersen A, Sandström B, Van Amelsvoort JMM. The effect of ingestion of inulin on blood lipids and gastrointestinal symptoms in healthy females. *British Journal of Nutrition*. 1997;78(2):215-222. doi:10.1079/bjn19970141
116. Dalile B, La Torre D, Kalc P, et al. Extruded Wheat Bran Consumption Increases Serum Short-Chain Fatty Acids but Does Not Modulate Psychobiological Functions in Healthy Men: A Randomized, Placebo-Controlled Trial. *Front Nutr*. 2022;9. doi:10.3389/fnut.2022.896154
117. Wang S, Mu L, Yu C, et al. Microbial collaborations and conflicts: unraveling interactions in the gut ecosystem. *Gut Microbes*.*Taylor and Francis Ltd.* 2024;16(1). doi:10.1080/19490976.2023.2296603
118. Takada T, Kurakawa T, Tsuji H, Nomoto K. Fusicatenibacter saccharivorans gen. nov., sp. nov., isolated from human faeces. *Int J Syst Evol Microbiol*. 2013;63(PART10):3691-3696. doi:10.1099/ijs.0.045823-0
119. Li J, Zhu S, Wang Y, et al. Metagenomic association analysis of cognitive impairment in community-dwelling older adults. *Neurobiol Dis*. 2023;180. doi:10.1016/j.nbd.2023.106081
120. Loh JS, Mak WQ, Tan LKS, et al. Microbiota–gut–brain axis and its therapeutic applications in neurodegenerative diseases. *Signal Transduct Target Ther*.*Springer Nature*. 2024;9(1). doi:10.1038/s41392-024-01743-1

1117 **Tables**

1118 **Table 1.** Baseline demographic and clinical characteristics of participants randomized to
1119 treatment counterbalanced.
1120

	Overall N = 42	**CON** N = 21	**SCF** N = 21
Education			
High School Graduate	2 (4.8%)	0 (0%)	2 (9.5%)
Some college	6 (14%)	3 (14%)	3 (14%)
Bachelor's Degree	13 (31%)	8 (38%)	5 (24%)
Advanced Degree	21 (50%)	10 (48%)	11 (52%)
Ethnicity			
Asian	6 (14%)	3 (14%)	3 (14%)
Black or African American	3 (7.1%)	1 (4.8%)	2 (9.5%)
Mixed or Other	1 (2.4%)	0 (0%)	1 (4.8%)
White (Caucasian)	32 (76%)	17 (81%)	15 (71%)
Latino	1 (2.4%)	1 (4.8%)	0 (0%)
Sex			
Female	28 (67%)	15 (71%)	13 (62%)
Male	14 (33%)	6 (29%)	8 (38%)
Age (years)	56.2 ± 7.3	54.8 ± 6.2	57.5 ± 8.2
Fiber per 1000kcal	11.4 ± 3.4	12.0 ± 3.3	10.8 ± 3.5
BMI (kg/m²)	25.9 ± 4.0	25.4 ± 3.7	26.3 ± 4.2
Income			
<$31,000-40,000	3 (9.5%)	1 (4.8%)	2 (14.3%)
$41,000-50,000	3 (7.1%)	1 (4.8%)	2 (9.5%)
$51,000-60,000	3 (7.1%)	2 (9.5%)	1 (4.8%)
$61,000-70,000	4 (9.5%)	1 (4.8%)	3 (14%)
$71,000-80,000	5 (12%)	4 (19%)	1 (4.8%)
$81,000-90,000	1 (2.4%)	1 (4.8%)	0 (0%)
$91,000-100,000	7 (16.7%)	4 (19%)	3 (14%)
Greater than $100,000	15 (35.7%)	7 (33%)	8 (38%)

1121
1122 Baseline characteristics of participants enrolled and randomized into the clinical trial (N = 42), grouped by initial
1123 treatment assignment. Dietary fiber (g/1000 kcal) values reflect baseline intake assessed using DHQ3 prior to the first
1124 intervention period. Height and weight were measured at the baseline visit and used to calculate body mass index
1125 (BMI; kg/m^2). Continuous variables are reported as mean ± standard deviation; categorical variables are reported as
1126 number of participants and percentage within each group [n (%)].
1127

1128

Table 2. Behavioral and ERP measures during the flanker task across treatment and time.

	Maltodextrin		Soluble Corn Fiber					
	PRE	POST	PRE	POST	Treatment Effect (ΔSCF - ΔCON)			
Behavioral Flanker	Mean ± SEM *(n)*	Mean ± SEM *(n)*	Mean ± SEM *(n)*	Mean ± SEM *(n)*	β	SE	95% CI	*p*
Accuracy (%)								
Congruent	96.9 ± 0.52 *(39)*	95.5 ± 1.37 *(39)*	97.0 ± 0.48 *(40)*	97.6 ± 0.45 *(40)*	0.65	0.8	[-0.93, 2.23]	0.42
Incongruent	92.4 ± 1.00 *(39)*	92.0 ± 1.53 *(39)*	93.6 ± 0.79 *(40)*	94.4 ± 0.70 *(40)*	-0.68	1.1	[-2.82, 1.46]	0.53
Reaction Time (ms)								
Congruent	395. ± 5.79 *(39)*	**398. ± 6.69**[a] *(39)*	400.71 ± 6.22 *(40)*	**389. ± 5.52**[b] *(40)*	-18.4	4.2	[-18.4, -1.2]	**0.01***
Incongruent	431. ± 6.62 *(39)*	**437. ± 7.77**[a] *(39)*	435.43 ± 6.88 *(40)*	**424. ± 6.35**[b] *(40)*	-14.2	4.4	[-22.8, -5.6]	**0.003****
ERP Flanker								
Amplitude (μV)								
Congruent	5.96 ± 1.73 *(39)*	6.78 ± 0.68 *(36)*	6.64 ± 0.60 *(39)*	7.07 ± 0.77 *(37)*	0.88	1.18	[-2.22, 1.01]	0.46
Incongruent	6.36 ± 1.64 *(39)*	6.77 ± 0.69 *(36)*	7.14 ± 0.65 *(39)*	7.50 ± 0.79 *(37)*	1.08	1.10	[-1.06, 3.24]	0.33
Peak Latency (ms)								
Congruent	386. ± 6.71 *(39)*	399. ± 10.18 *(36)*	394. ± 7.29 *(39)*	398. ± 7.99 *(37)*	-6.16	0.32	[-31.1, 18.7]	0.67
Incongruent	424. ± 8.34 *(39)*	443. ± 11.70 *(36)*	438. ± 9.90 *(39)*	429. ± 8.27 *(37)*	-23.0	15.4	[-53.2, 6.81]	0.14

Values are means ± standard error of the mean (SEM) and sample size (n) across congruencies at each timepoint. Measures include accuracy (%), reaction time (ms), P3 amplitude (μV), and P3 peak latency (ms). Linear mixed-effect models included participant ID as a random effect, and the fixed effects of treatment, time, and their interaction. Reported are the treatment-by-time interaction estimates (β, Standard Error (SE), 95% confidence interval (CI), *p*-values). Pairwise comparisons were conducted within each congruency when a treatment-by-time interaction met the significance threshold ($P < 0.05$), with *p*-values adjusted using the Benjamin-Hochberg procedure. Superscripts (a, b) denote significant *pairwise* differences within congruency trials between treatments and time. Significance threshold *p*: '**' <0.01, '*' <0.05, '†' <0.1.

Table 3. 16S Alpha diversity and differential abundance of genera across intervention periods.

	Maltodextrin		Soluble Corn Fiber					
	PRE	POST	PRE	POST	Treatment Effect (ΔSCF - ΔCON)			
16S ASVs	Mean ± SEM *(n)*	Mean ± SEM *(n)*	Mean ± SEM *(n)*	Mean ± SEM *(n)*	β	SE	95% CI	FDR *P*
Genera (% of sequence)								
Bacteroides	25.2 ± 1.77 *(38)*	23.7 ± 1.90 *(38)*	27.3 ± 2.06 *(37)*	22.6 ± 2.07 *(37)*	-0.15	0.10	[-0.34, 0.05]	0.11
Faecalibacterium	10.2 ± 1.02 *(38)*	10.1 ± 1.11 *(38)*	8.66 ± 1.15 *(37)*	11.0 ± 1.30 *(37)*	0.23	0.21	[-0.18, 0.64]	0.47
Parabacteroides	2.52 ± 0.35[a] *(38)*	**2.06 ± 0.24[a]** *(38)*	2.09 ± 0.26[a] *(37)*	**8.37 ± 0.98[b]** *(37)*	1.44	0.22	[1.01, 1.88]	**<0.001*** **
Alistipes	3.46 ± 0.51 *(38)*	2.82 ± 0.35 *(38)*	3.88 ± 0.59 *(37)*	3.96 ± 0.69 *(37)*	0.08	0.20	[-0.31, 0.46]	0.50
Blautia	3.76 ± 0.50 *(38)*	4.52 ± 0.61 *(38)*	3.54 ± 0.42 *(37)*	3.24 ± 0.50 *(37)*	-0.27	0.13	[-0.52, -0.02]	0.10†
Agathobacter	4.16 ± 0.88 *(38)*	5.97 ± 1.17 *(38)*	3.99 ± 0.85 *(37)*	2.80 ± 0.58 *(37)*	-0.46	0.23	[-0.91, 0.01]	0.11
Subdoligranulum	2.31 ± 0.29 *(38)*	2.54 ± 0.38 *(38)*	3.24 ± 0.58 *(37)*	2.69 ± 0.49 *(37)*	-0.24	0.22	[-0.68, 0.19]	0.83
Prevotella	0.87 ± 0.41 *(38)*	1.64 ± 0.74 *(38)*	1.60 ± 0.89 *(37)*	2.13 ± 1.04 *(37)*	-0.22	0.30	[-0.81, 0.37]	0.53
Dialister	1.34 ± 0.44[a] *(38)*	**1.46 ± 0.51[a]** *(38)*	0.93 ± 0.34[a] *(37)*	**2.10 ± 0.63[b]** *(37)*	1.06	0.39	[0.29, 1.83]	**0.02***
Bifidobacterium	2.50 ± 0.53 *(38)*	2.69 ± 0.53 *(38)*	2.12 ± 0.52 *(37)*	2.09 ± 0.41 *(37)*	0.09	0.31	[-0.51, 0.70]	0.92
Fusicatenibacter	0.60 ± 0.10[a] *(38)*	**0.67 ± 0.09[a]** *(38)*	0.53 ± 0.11[a] *(37)*	**1.79 ± 0.28[b]** *(37)*	1.10	1.10	[0.59, 1.61]	**<0.001*** **
Alpha Diversity Metrics								
Richness	439.9 ± 19.8[a] *(38)*	**438.7 ± 18.2[a]** *(38)*	443.6 ± 17.6[a] *(37)*	**413.7 ± 18.6[b]** *(37)*	-0.76	0.29	[-1.32, -0.19]	**0.03***
Shannon	3.89 ± 0.06 *(38)*	3.88 ± 0.06 *(38)*	3.81 ± 0.06 *(37)*	3.71 ± 0.07 *(37)*	-0.08	0.07	[-0.22, 0.06]	0.26
Faith's PD	104.7 ± 1.62 *(38)*	103.9 ± 1.54 *(38)*	105.23 ± 1.54 *(37)*	101.9 ± 1.80 *(37)*	-2.43	1.28	[-4.93, 0.06]	0.09†

Values are means ± standard error of the mean (SEM) and sample size (*n*) across each timepoint. For differential abundance of 16S genera, a generalized linear mixed-effect negative binomial model included participant ID as a random effect, and the fixed effects of treatment, time, and their interaction. Reported are the treatment-by-time interaction log-scaled estimates (β, Standard Error (SE), 95% confidence interval (CI), FDR-adjusted *p*-values). For alpha diversity metrics, linear mixed-effect model. Reported are the treatment-by-time interaction estimates. Pairwise comparisons was conducted if an interaction *(treatment effect)* met the significance threshold ($P < 0.05$), *p*-values adjusted using the Benjamin-Hochberg procedure. Superscripts (a, b) denote significant *pairwise* treatment effect. Significance threshold *p*: '***' <0.001, '**' <0.01, '*' <0.05, '†' <0.1.

1147 **Table 4.** Fecal volatile fatty acids across the intervention periods.

	Maltodextrin		Soluble Corn Fiber					
	PRE	**POST**	**PRE**	**POST**	**Treatment Effect (ΔSCF - ΔCON)**			
Fermentation end-products (μmol/g DMB)	Mean ± SEM *(n)*	Mean ± SEM *(n)*	Mean ± SEM *(n)*	Mean ± SEM *(n)*	β	SE	95% CI	*P*
SCFAs								
Butyrate	43.3 ± 4.56 *(38)*	43.9 ± 5.26 *(37)*	38.8 ± 4.58 *(37)*	40.1 ± 3.18 *(37)*	0.10	0.13	[-0.16, 0.37]	0.44
Acetate	176. ± 13.9 *(38)*	182. ± 13.5 *(37)*	165. ± 13.2 *(37)*	202. ± 14.9 *(37)*	0.16	0.11	[-0.04, 0.36]	0.14
Propionate	48.1 ± 3.98 *(38)*	50.8 ± 4.40 *(37)*	47.5 ± 4.32 *(37)*	55.6 ± 4.72 *(37)*	0.14	0.10	[-0.09, 0.36]	0.23
Total SCFAs	267. ± 21.5 *(38)*	273. ± 21.97 *(37)*	255. ± 20.6 *(37)*	298. ± 22.3 *(37)*	0.15	0.11	[-0.05, 0.36]	0.15
BCFAs								
Valerate	6.44 ± 0.59 *(38)*	5.99 ± 0.47 *(37)*	6.00 ± 0.47 *(37)*	5.68 ± 0.48 *(37)*	-0.06	0.16	[-0.36, 0.24]	0.71
Isobutyrate	6.62 ± 0.54 *(38)*	5.97 ± 0.39 *(36)*	6.29 ± 0.52 *(37)*	5.22 ± 0.33 *(37)*	-0.08	0.11	[-0.30, 0.14]	0.48
Isovalerate	9.49 ± 0.82 *(38)*	8.30 ± 0.57 *(36)*	8.66 ± 0.69 *(37)*	7.35 ± 0.54 *(37)*	-0.04	0.14	[-0.31, 0.22]	0.75
Total BCFAs	22.6 ± 1.83 *(38)*	20.4 ± 1.31 *(37)*	21.0 ± 1.56 *(37)*	18.3 ± 1.14 *(37)*	-0.03	0.20	[-0.43, 0.36]	0.87

1148
1149 Values are descriptive means ± standard error of the mean (SEM) and sample size (n) across each timepoint. Total SCFAs and BCFAs are pooled measures, within
1150 respective category, concentrations are on a dry matter basis (DMB). Linear mixed-effect models included participant ID as a random effect, and the fixed effects
1151 of treatment, time, and their interaction (Treatment Effect). Reported are the treatment-by-time interaction estimates (β, Standard Error (SE), 95% confidence
1152 interval (CI), *p*-values).

1153 **Table 5.** Self-reported gastrointestinal symptom severity scores across the intervention.

	Maltodextrin		**Soluble Corn Fiber**		
	PRE	**POST**	**PRE**	**POST**	
GI Symptoms	Median [IQR] *(n)*	Median [IQR] *(n)*	Median [IQR] *(n)*	Median [IQR] *(n)*	*P*
Gas	1.57 [0.84] *(39)*	**1.43 [1.00]** *(39)*	1.57 [0.97] *(38)*	**1.93 [1.00]** *(38)*	**0.01***
Cramping	1.00 [0.00] *(39)*	1.00 [0.00] *(39)*	1.00 [0.00] *(38)*	1.00 [0.14] *(38)*	0.91
Bloating	1.00 [0.14] *(39)*	1.00 [0.14] *(39)*	1.00 [0.14] *(38)*	1.00 [0.32] *(38)*	0.05†
Nausea	1.00 [0.00] *(39)*	1.00 [0.00] *(39)*	1.00 [0.00] *(38)*	1.00 [0.00] *(38)*	0.17
Reflux	1.00 [0.00] *(39)*	1.00 [0.00] *(39)*	1.00 [0.03] *(38)*	1.00 [0.00] *(38)*	0.84
Rumbling	1.00 [0.16] *(39)*	1.00 [0.16] *(39)*	1.00 [0.17] *(38)*	1.00 [0.41] *(38)*	0.68
Burping	1.00 [0.16] *(39)*	1.00 [0.00] *(39)*	1.00 [0.28] *(38)*	1.00 [0.17] *(38)*	0.70

1154
1155 Values are median [interquartile range (IQR)] and sample size (n) at each timepoint. Symptom were rated on a 4-point
1156 scale (1 = Absent, 2 = Mild, 3 = Moderate, 4 = Severe). Reported values include *p*-values from the paired Wilcoxon
1157 Signed-Rank testing the treatment effect on change over time using delta values. Significance threshold *p*: '*' <0.05,
1158 '†' <0.1.
1159

1160

1161

1162

1163

1164

1165

1166

1167

1168

1169 **Table 6.** Mediation of SCF-related changes in Flanker reaction times through fecal SCFAs and
1170 16S genera.

			Nonparametric Bootstrap Confidence Intervals with Percentile		
Mediator	**Flanker Task**	**Effect**	**β**	**[95% CI]**	***P***
Acetate	Congruent RT	ACME	-0.57	[-2.51, 0.87]	0.48
		ADE	-13.42	[-23.7, -3.23]	0.01*
		Total effect	-13.99	[-24.4, -14.0]	0.009**
		Proportion Mediated	4.09%	[-0.08, 0.21]	0.48
	Incongruent RT	ACME	-0.44	[-2.87, 1.61]	0.72
		ADE	-17.03	[-29.4, -4.38]	0.008**
		Total effect	-17.47	[-30.1, -4.63]	0.007**
		Proportion Mediated	2.51%	[-0.11, 0.19]	0.72
Propionate	Congruent RT	ACME	-0.64	[-2.39, 0.81]	0.43
		ADE	-13.39	[-23.9, -3.30]	0.01*
		Total effect	-14.03	[-24.4, -3.78]	0.008**
		Proportion Mediated	4.57%	[-0.28, 0.08]	0.43
	Incongruent RT	ACME	-0.38	[-4.32, 0.78]	0.22
		ADE	-17.11	[-23.0, -2.36]	0.03*
		Total effect	-17.49	[-24.3, -3.77]	0.01*
		Proportion Mediated	2.22%	[-0.11, 0.54]	0.23
Parabacteroides	Congruent RT	ACME	-0.15	[-9.31, 4.27]	0.93
		ADE	-13.85	[-25.9, 0.39]	0.06
		Total effect	-14.00	[-24.3, -3.83]	0.008**
		Proportion Mediated	1.06%	[-0.36, 1.02]	0.93
	Incongruent RT	ACME	-0.48	[-12.64, 4.53]	0.86
		ADE	-17.00	[-30.5, 0.20]	0.03*
		Total effect	-17.48	[-30.0, -4.80]	0.01*
		Proportion Mediated	2.75%	[-0.34, 0.96]	0.86
Fusicatenibacter	Congruent RT	ACME	-1.40	[-4.98, 0.65]	0.19
		ADE	-12.63	[-23.0, -2.28]	0.02*
		Total effect	-14.03	[-24.3, -3.84]	0.007**
		Proportion Mediated	10.0%	[-0.06, 0.50]	0.19
	Incongruent RT	ACME	-0.72	[-4.98, 2.16]	0.59
		ADE	-16.75	[-29.1, -3.85]	0.01*
		Total effect	-17.47	[-30.0, -4.79]	0.007**
		Proportion Mediated	4.1%	[-0.18, 0.35]	0.59
Dialister	Congruent RT	ACME	0.44	[-0.89, 3.47]	0.52
		ADE	-14.44	[-25.4, -4.22]	0.006**
		Total effect	-14.00	[-24.2, -3.75]	0.007**
		Proportion Mediated	-3.15%	[-0.33, 0.08]	0.53
	Incongruent RT	ACME	0.67	[-1.26, 4.95]	0.52
		ADE	-18.15	[-31.8, -5.12]	0.007**
		Total effect	-17.49	[-30.0, -4.70]	0.007**
		Proportion Mediated	-3.8%	[-0.35, 0.11]	0.53

1171 Mediation analysis ($n = 37$) was conducted using nonparametric bootstrapped linear regression models (R; *mediation*)
1172 to estimate the average causal mediation effect (ACME), average direct effect (ADE), and total effects of treatment
1173 on changes in reaction times (RT) Reported are the model estimates (β), Standard Error (SE), 95% confidence interval
1174 (CI). Proportion mediated indicates the percentage of the total effect explained by the ACME pathway. Significance
1175 threshold *p*: '***' <0.001, '**' <0.01, '*' <0.05, '†' <0.1.

Table 7. Moderation of the SCF effect on change in flanker reaction time by change in 16S genera and fecal metabolites

Moderator	Flanker Task	Treatment x Moderator (Model Summary)						
		ΔR^2	Adj. ΔR^2	β	SE	t	[95% CI]	*P*
Acetate	Congruent RT	0.11	0.07	3.13	5.62	0.56	[-8.08, 14.3]	0.58
	Incongruent RT	0.10	0.06	2.21	6.80	0.33	[-11.4, 15.8]	0.75
Propionate	Congruent RT	0.11	0.07	0.43	5.60	0.08	[-10.76, 11.6]	0.94
	Incongruent RT	0.10	0.06	0.40	6.80	0.06	[-13.17, 14.0]	0.95
Parabacteroides	Congruent RT	**0.16**	0.12	**-19.8**	10.12	-1.95	[-40.0, 0.43]	**0.05***
	Incongruent RT	**0.15**	0.12	**-25.1**	12.24	-2.05	[-49.5, 0.63]	**0.04***
Fusicatenibacter	Congruent RT	0.10	0.06	-1.31	13.48	-0.10	[-28.2, 25.6]	0.92
	Incongruent RT	0.11	0.07	11.49	16.20	0.71	[-20.9, 43.8]	0.49
Dialister	Congruent RT	0.11	0.07	-4.49	7.39	-0.61	[-19.2, 10.3]	0.55
	Incongruent RT	0.10	0.06	0.23	8.98	0.03	[-17.7, 18.2]	0.98

Moderation analysis (n = 37) was tested using linear regression models testing if changes in moderators explain variability in flanker reaction times (RT). Each model includes treatment, Δ moderator, and its interaction. Reported are the treatment-by-moderator estimates (β, Standard Error (SE), 95% confidence interval (CI), p-values). The ΔR^2 and adjusted ΔR^2 columns show the variance explained by the full model. Statistical threshold for p: '***' <0.001, '**' <0.01, '*' <0.05, '†' <0.1.

1190 **Table 8.** Responder vs. non-responder descriptive summary during the SCF intervention period

	Non-Responder		**Responder**	
	PRE	**POST**	**PRE**	**POST**
Pilot Analyses	Mean ± SD *(n)*	Mean ± SD *(n)*	Mean ± SD *(n)*	Mean ± SD *(n)*
Genera (% of Sequences)				
Parabacteroides	0.43 ± 0.64 *(3)*	*ND (3)*	1.04 ± 0.33 *(3)*	14.61 ± 2.82 *(3)*
Dialister	1.50 ± 0.79 *(3)*	3.18 ± 3.25 *(3)*	0.25 ± 0.43 *(3)*	*ND (3)*
Fusicatenibacter	0.48 ± 0.45 *(3)*	2.69 ± 2.77 *(3)*	1.24 ± 1.65 *(3)*	1.35 ± 1.34 *(3)*
Species (% of Sequences)				
P. distasonis	0.01 ± 0.01 *(3)*	*ND (3)*	0.49 ± 0.17 *(3)*	11.38 ± 1.47 *(3)*
P. merdae	0.41 ± 0.63 *(3)*	*ND (3)*	0.55 ± 0.50 *(3)*	3.23 ± 3.67 *(3)*
P. faecis	0.01 ± 0.01 *(3)*	*ND (3)*	*ND (3)*	*ND (3)*
D. invisus	0.73 ± 0.73 *(3)*	1.00 ± 1.74 *(3)*	0.25 ± 0.43 *(3)*	*ND (3)*
D. hominis	0.77 ± 1.34 *(3)*	2.17 ± 3.75 *(3)*	*ND (3)*	*ND (3)*
F. saccharivorans	0.48 ± 0.45 *(3)*	2.69 ± 2.77 *(3)*	1.24 ± 1.65 *(3)*	1.35 ± 1.34 *(3)*
Flanker Reaction Time (ms)				
Congruent	428.9 ± 24.4 *(3)*	396.7 ± 11.6 *(3)*	363.0 ± 50.2 *(3)*	362.1 ± 42.7 *(3)*
Incongruent	456.6 ± 3.9 *(3)*	424.9 ± 14.4 *(3)*	403.9 ± 60.2 *(3)*	401.1 ± 50.2 *(3)*
SCFAs (µmol/g DMB)				
Acetate	153.8 ± 60.9 *(3)*	225.4 ± 88.9 *(3)*	180.2 ± 95.1 *(3)*	246.6 ± 59.1 *(3)*
Propionate	28.47 ± 12.2 *(3)*	57.02 ± 23.7 *(3)*	51.89 ± 23.6 *(3)*	72.81 ± 27.2 *(3)*
Demographics				
Age *(year)*	53.7 ± 7.2 *(3)*		54.3 ± 2.5 *(3)*	

1191
1192 Responders (n=3) and non-responders (n=3) following the SCF intervention. Responders were the three participants
1193 with the largest increase in *Parabacteroides* (16S) following SCF; non-responders were the three participants with the
1194 smallest change following SCF (total N = 6 participants). Data are presented as mean ± standard deviation (SD) and
1195 sample size (*n*). Genus and species relative abundances (%) were derived from shotgun metagenomic profiling using
1196 MetaPhlAn4. Species initials correspond as genus followed by species name: *P* = *Parabacteroides*, *D* = *Dialister*, and
1197 *F* = *Fusicatenibacter*. ND = not detected (no reads assigned at the reported taxonomic level.)
1198

1199

1200

1201 **Figure Legend**

1202 **Figure 1. CONSORT flow diagram of recruitment, randomization, and retention.**
1203 Participants were randomized (n=42) to start with either the maltodextrin control (CON) or soluble
1204 corn fiber (SCF) in Period 1, then crossed over to the alternate condition in Period 2 following
1205 washout. Boxes show the "*n*" indicating the number of participants at each stage and reasons for
1206 exclusion or missing data of the SCOPE study. (*Figure created using BioRender)*
1207
1208 **Figure 2. Soluble corn fiber (SCF) consumption improved flanker reaction times.** Observed
1209 reaction times (RT, millisecond) are shown at both time points for the maltodextrin control (CON)
1210 and SCF intervention periods for (**A**) congruent trials and (**B**) incongruent trials. Right panels
1211 display model-estimated marginal means (coefficients and the 95% confidence intervals for both
1212 congruent and incongruent trials (FDR corrected pairwise contrasts; symbols shown in right
1213 panels). Statistical significance derived from pairwise comparisons. FDR-adjusted *p*-values
1214 annotated as follows: ** < 0.01; * < 0.05.
1215
1216 **Figure 3. 16S microbiota composition across condition and participants.** (n=38 CON, n=37
1217 SCF). (**A**) Mean relative abundance (% of sequence) of the top 5 for phyla (*left*) and top 10 for
1218 genera (*right*) at PRE and POST for each intervention. Genus colors correspond to their parent
1219 phylum. (**B**) Differential abundance of genera from a generalized linear mixed model showing the
1220 treatment effect estimates with effect size increasing from the center dashed vertical line. The y-
1221 axis corresponds to the significance of the genera, higher meaning more significant, with a
1222 horizontal dashed line indicating the FDR P = 0.05 threshold. Individual participant-sample
1223 relative abundances are shown as a (**C**) waterfall of the distribution of SCF-responsive features.
1224 Incertae sedis is group of bacteria without taxonomical assignment.
1225
1226 **Figure 4. Interaction between 16S-derived Δ*Parabacteroides* and the SCF effect on flanker**
1227 **RT.** Panels show moderation results for (**A**) for congruent and (**B**) incongruent trials. The outcome
1228 is ΔRT (POST-PRE, ms), where negative values indicate faster RT. The moderator is
1229 Δ*Parabacteroides* (POST-PRE), mean-centered and z-scaled (negative values reflect smaller-
1230 than-average changes). Left panels show observed data and model-predicted simple slopes for
1231 CON (blue) and SCF (orange); vertical reference lines indicate -1 SD (standard deviation), average
1232 (0 SD), and +1 SD. Right panels show estimated SCF-CON emmeans contrasts in ΔRT at -1,0,
1233 and +1SD of Δ*Parabacteroides*; the vertical line at 0 indicates no difference. Statistical
1234 significance threshold p * <0.05.
1235
1236 **Figure 5. Growth rates of *Parabacteroides distasonis* cultured in M9 supplement with SCF**
1237 **compared to controls.** The relative log growth curve of *P. distasonis* (**A**) in M9 minimal medium
1238 supplemented with different carbohydrate sources. OD_0 represents the initial optical density
1239 (OD_{600}) at time zero. Each curve represents a mean biological replicate (N = 3), and error bars
1240 indicate propagated standard deviations. The mean growth rate (**B**), calculated as the slope of
1241 ln(OD) over sequential 2-hour intervals, cut off at 10-hrs. Bars represent average growth rate
1242 across replicates. Significance threshold p: '***' < 0.001, '**' < 0.01, '*' < 0.05, '†' < 0.1, 'NS'
1243 > 0.1.
1244

1245 **Figure 6. Exploratory responder analysis during the SCF period with MetaPhlAn4.** N = 6.
1246 Responders (n=3) were the participants with the largest *Parabacteroides* increase after SCF
1247 consumption, and non-responders (n=3) were the three with the smallest change (null/negative).
1248 The cognitive outcomes from the Flanker task demonstrate the responders (**A**) congruent and (**B**)
1249 incongruent reaction times (RT). Shotgun sequencing and MetaPhlan4 yielded (**C**) species
1250 resolution of microbial hits from 16S genus analysis. The bottom row demonstrates the diversity
1251 metrics for Alpha (**D**) richness and (**E**) Shannon evenness, and the principal coordinate analysis of
1252 (**F**) Beta diversity is shown using Bray-Curtis with adonis2 PERMANOVA values.

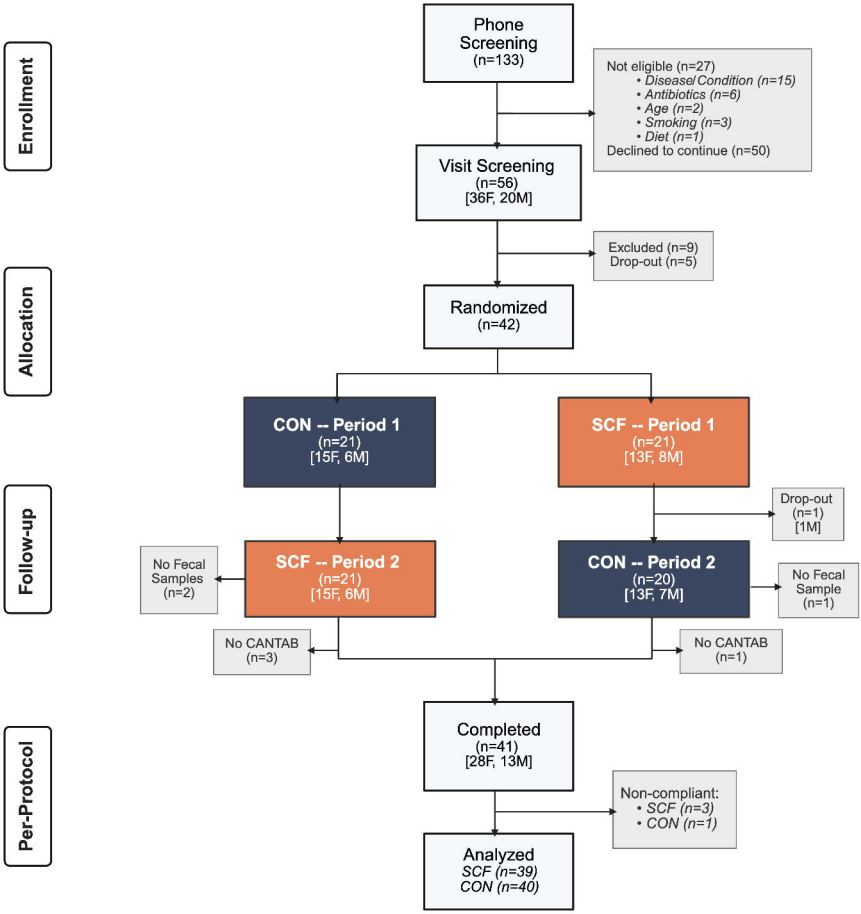
Enrollment
Allocation
Follow-up
Per-Protocol
Phone Screening (n=133)
Not eligible (n=27)
• Disease/Condition (n=15)
• Antibiotics (n=6)
• Age (n=2)
• Smoking (n=3)
• Diet (n=1)
Declined to continue (n=50)
Visit Screening (n=56) [36F, 20M]
Excluded (n=9)
Drop-out (n=5)
Randomized (n=42)
CON -- Period 1 (n=21) [15F, 6M]
SCF -- Period 1 (n=21) [13F, 8M]
Drop-out (n=1) [1M]
SCF -- Period 2 (n=21) [15F, 6M]
No Fecal Samples (n=2)
CON -- Period 2 (n=20) [13F, 7M]
No Fecal Sample (n=1)
No CANTAB (n=3)
No CANTAB (n=1)
Completed (n=41) [28F, 13M]
Non-compliant:
• SCF (n=3)
• CON (n=1)
Analyzed
SCF (n=39)
CON (n=40)

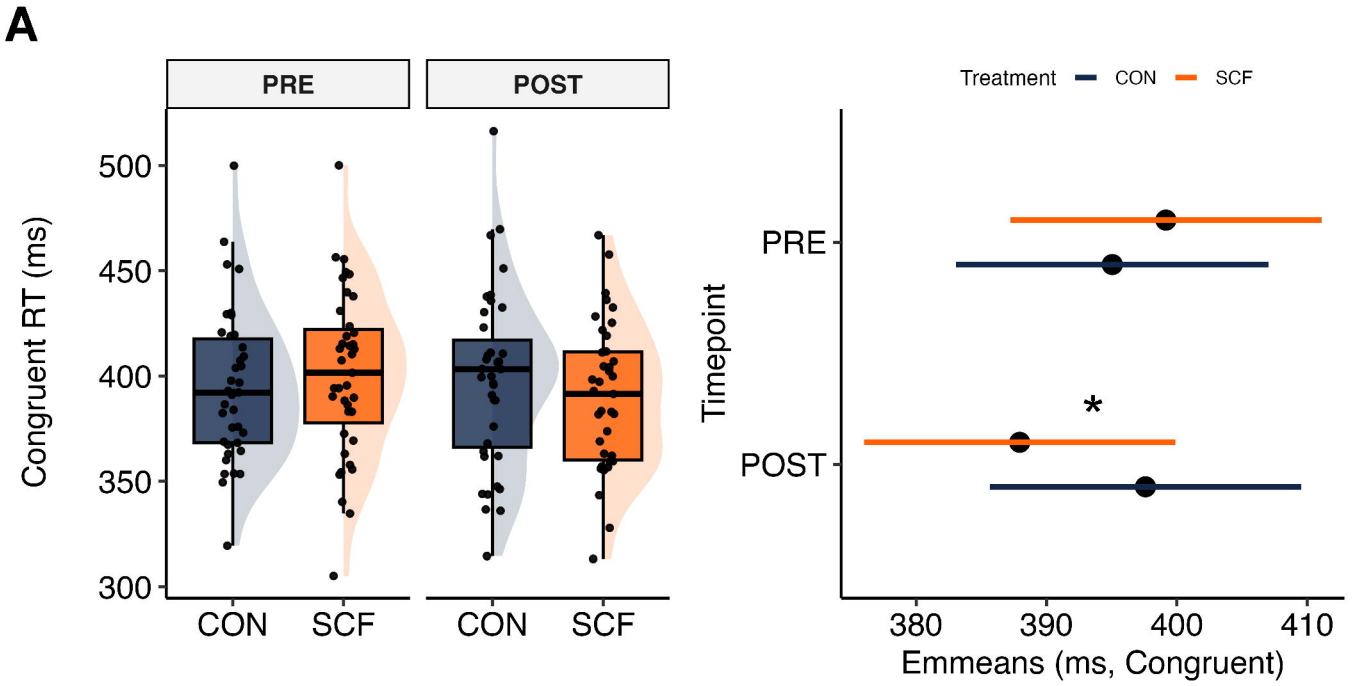
A
PRE
POST
Congruent RT (ms)
500
450
400
350
300
CON
SCF
CON
SCF
Treatment
CON
SCF
Timepoint
PRE
POST
*
380
390
400
410
Emmeans (ms, Congruent)

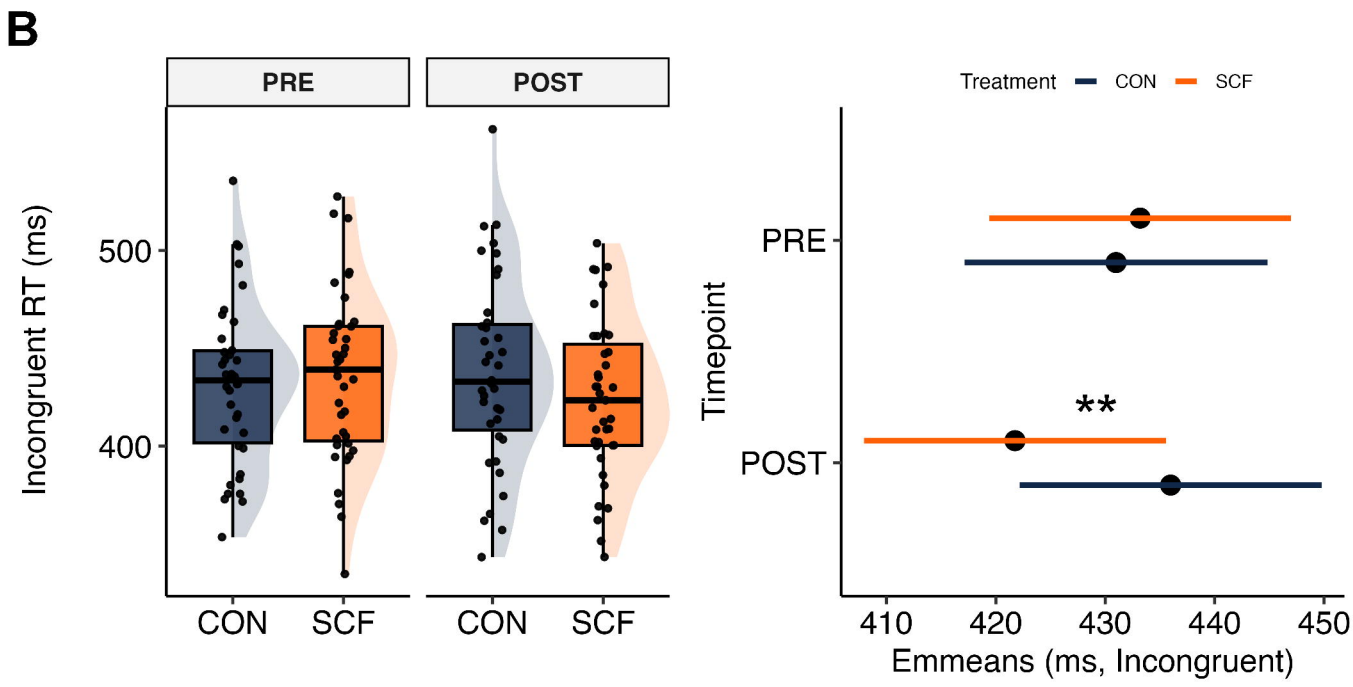
B
PRE
POST
Incongruent RT (ms)
500
400
CON
SCF
CON
SCF
Treatment
CON
SCF
Timepoint
PRE
POST
**
410
420
430
440
450
Emmeans (ms, Incongruent)

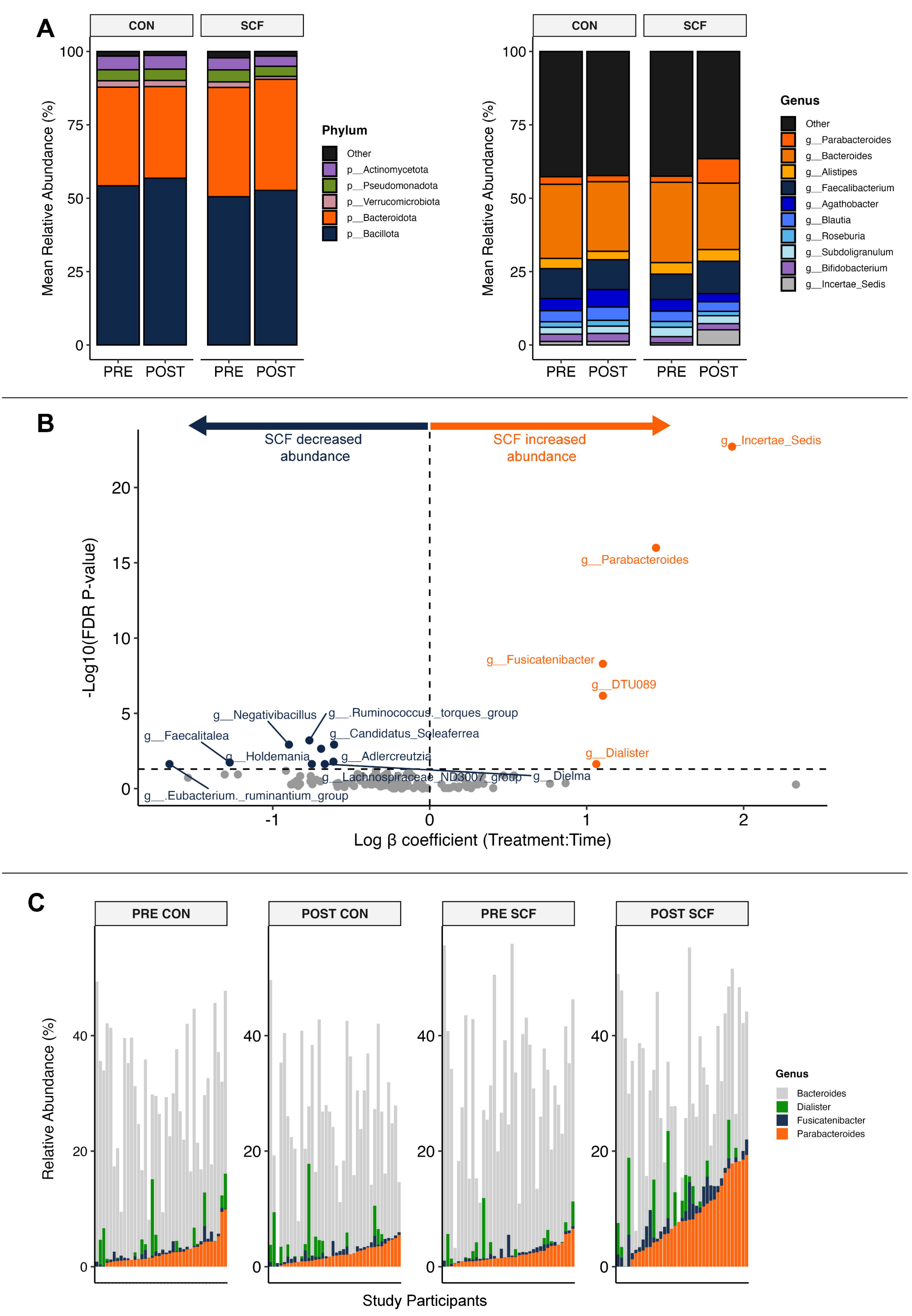
A
CON
SCF
Mean Relative Abundance (%)
100
75
50
25
0
PRE
POST
Phylum
Other
p__Actinomycetota
p__Pseudomonadota
p__Verrucomicrobiota
p__Bacteroidota
p__Bacillota
Genus
Other
g__Parabacteroides
g__Bacteroides
g__Alistipes
g__Faecalibacterium
g__Agathobacter
g__Blautia
g__Roseburia
g__Subdoligranulum
g__Bifidobacterium
g__Incertae_Sedis
B
SCF decreased abundance
SCF increased abundance
-Log10(FDR P-value)
20
15
10
5
0
-1
0
1
2
Log β coefficient (Treatment:Time)
g__Incertae_Sedis
g__Parabacteroides
g__Fusicatenibacter
g__DTU089
g__Dialister
g__Negativibacillus
g__.Ruminococcus._torques_group
g__Faecalitalea
g__Candidatus_Soleaferrea
g__Holdemania
g__Adlercreutzia
g__Lachnospiraceae_ND3007_group
g__Dielma
g__.Eubacterium._ruminantium_group
C
PRE CON
POST CON
PRE SCF
POST SCF
Relative Abundance (%)
40
20
0
Study Participants
Genus
Bacteroides
Dialister
Fusicatenibacter
Parabacteroides

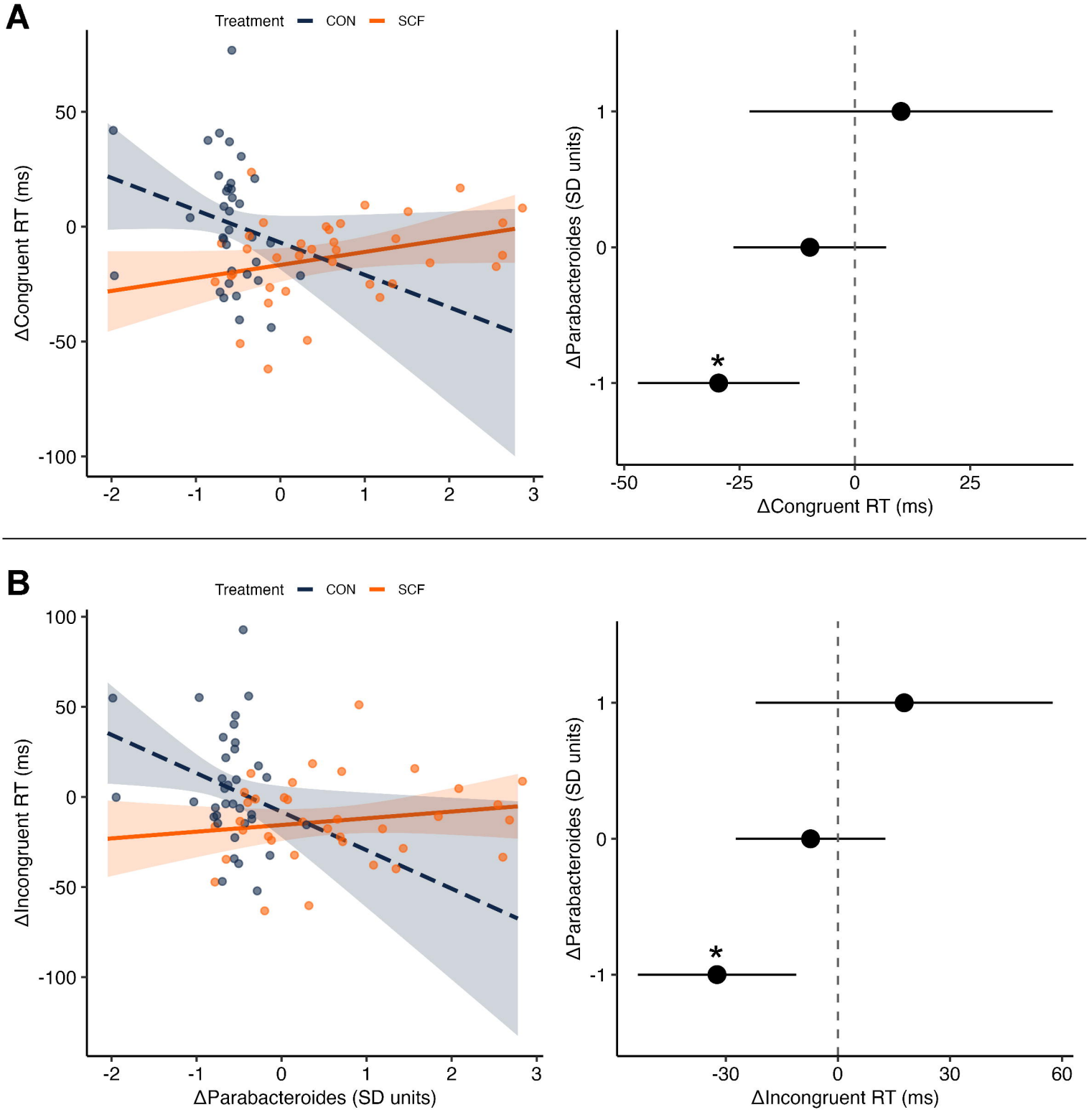
A
Treatment
CON
SCF
ΔCongruent RT (ms)
50
0
-50
-100
-2
-1
0
1
2
3
ΔParabacteroides (SD units)
1
0
-1
*
-50
-25
0
25
ΔCongruent RT (ms)
B
Treatment
CON
SCF
ΔIncongruent RT (ms)
100
50
0
-50
-100
-2
-1
0
1
2
3
ΔParabacteroides (SD units)
ΔParabacteroides (SD units)
1
0
-1
*
-30
0
30
60
ΔIncongruent RT (ms)

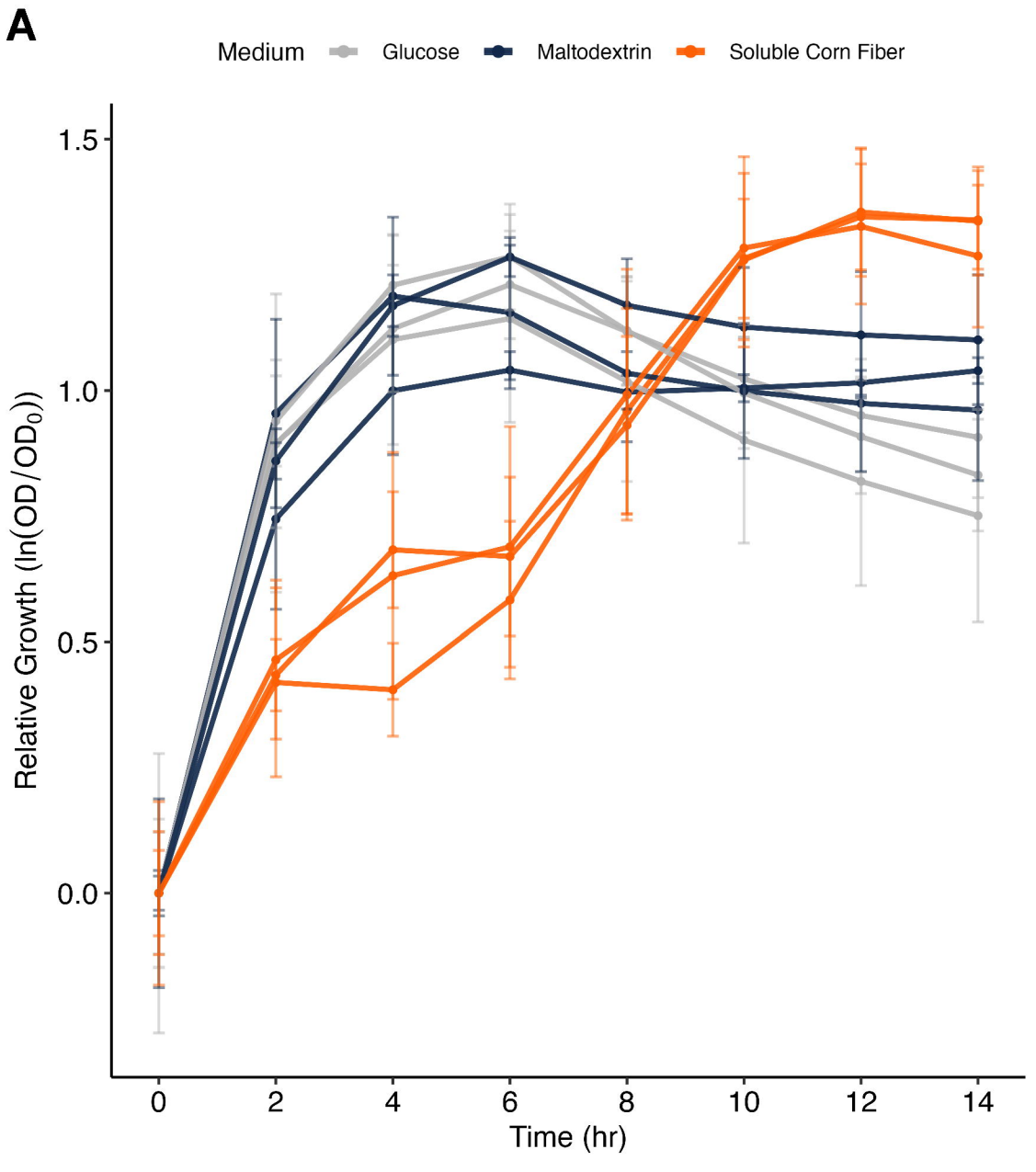
A
Medium
Glucose
Maltodextrin
Soluble Corn Fiber
Relative Growth (ln(OD/OD0))
1.5
1.0
0.5
0.0
0
2
4
6
8
10
12
14
Time (hr)

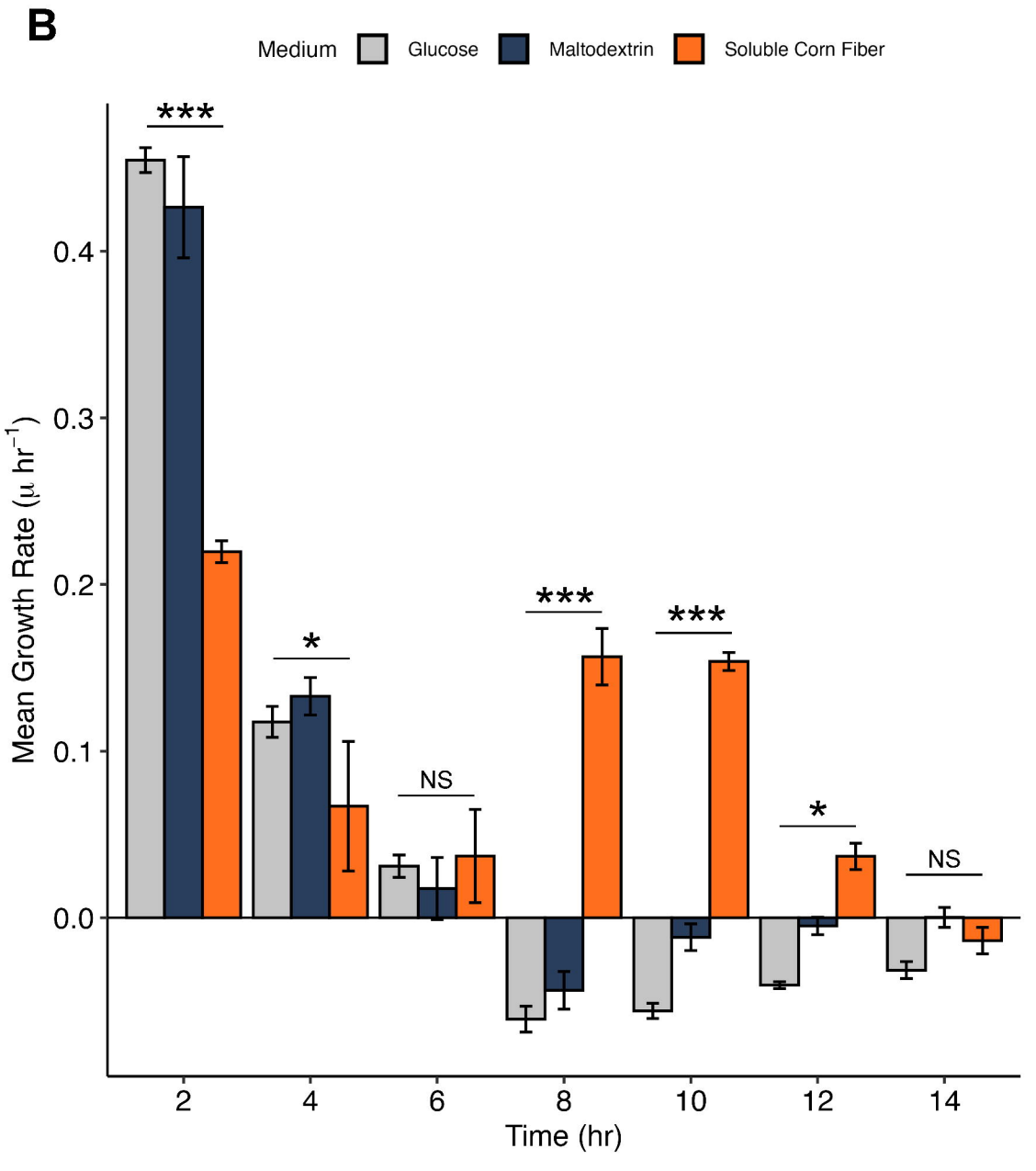
B
Medium
Glucose
Maltodextrin
Soluble Corn Fiber
Mean Growth Rate (μ hr-1)
0.4
0.3
0.2
0.1
0.0
***
*
NS
***
***
*
NS
2
4
6
8
10
12
14
Time (hr)

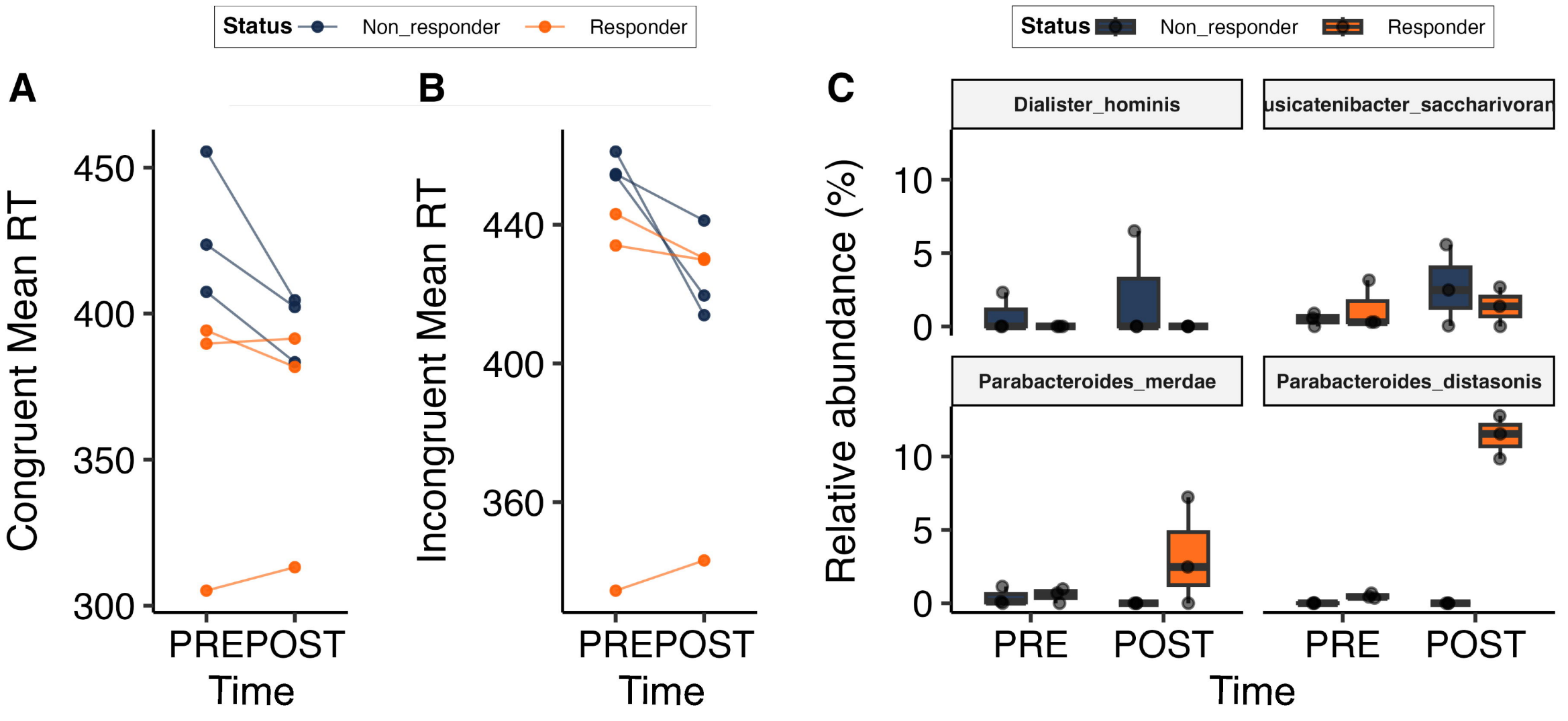
Status
Non_responder
Responder
A
Congruent Mean RT
450
400
350
300
PREPOST
Time
B
Incongruent Mean RT
440
400
360
PREPOST
Time
C
Dialister_hominis
usicatenibacter_saccharivoran
Parabacteroides_merdae
Parabacteroides_distasonis
Relative abundance (%)
10
5
0
PRE
POST
Time

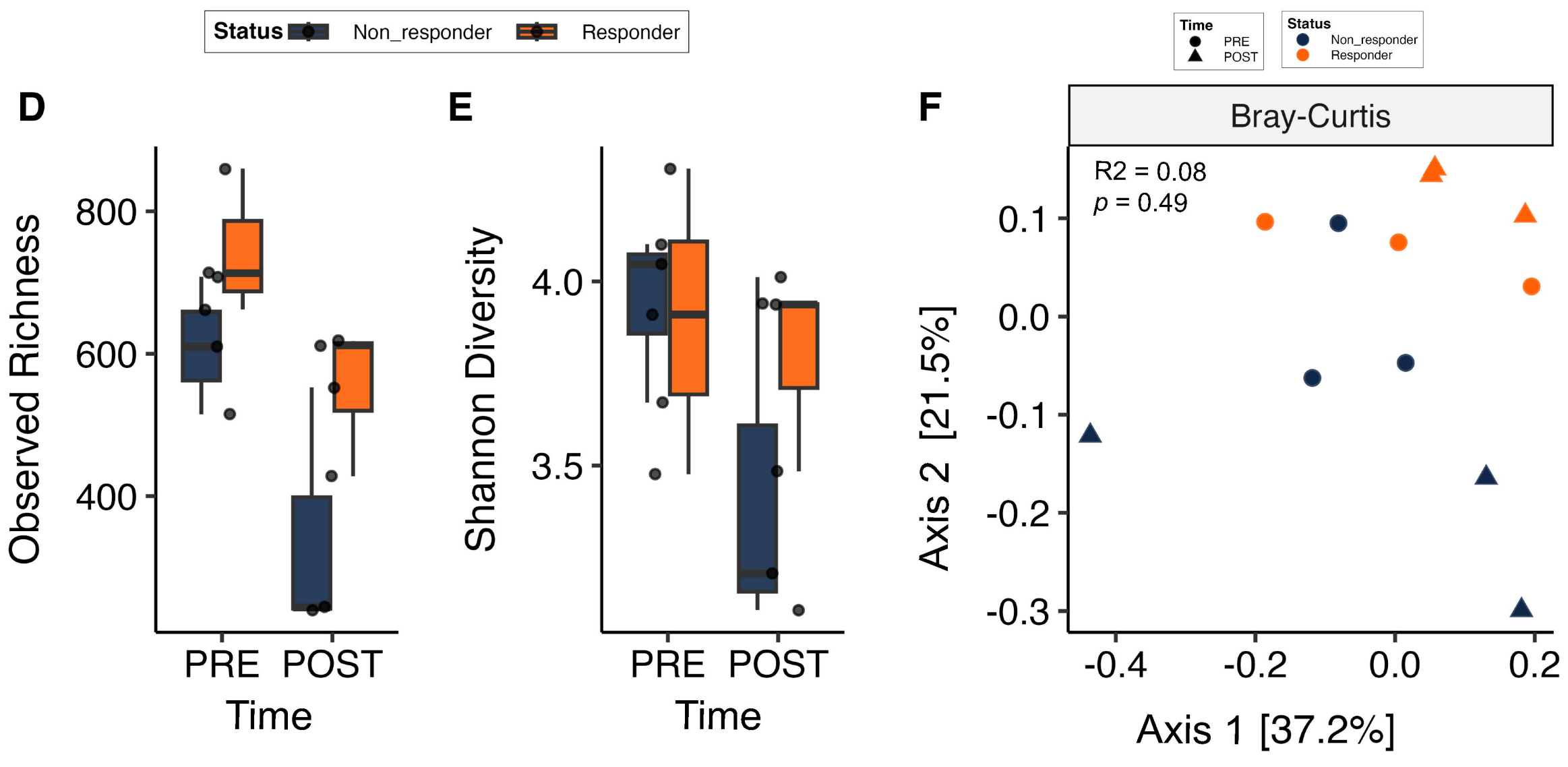
Status
Non_responder
Responder
D
Observed Richness
800
600
400
PRE
POST
Time
E
Shannon Diversity
4.0
3.5
PRE
POST
Time
Time
PRE
POST
Status
Non_responder
Responder
F
Bray-Curtis
R2 = 0.08
p = 0.49
Axis 2 [21.5%]
0.1
0.0
-0.1
-0.2
-0.3
-0.4
-0.2
0.0
0.2
Axis 1 [37.2%]